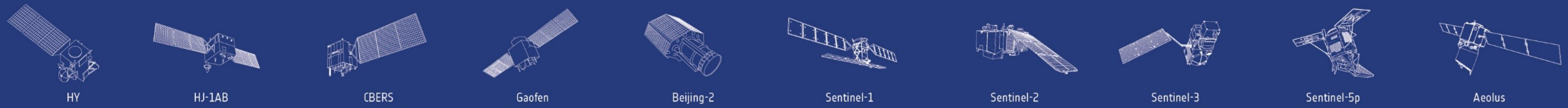

2023 DRAGON 5 SYMPOSIUM

3rd YEAR RESULTS REPORTING

11-15 SEPTEMBER 2023

[PROJECT ID. 59089]

[LIDAR OBSERVATIONS FROM ESA´S AEOLUS (WIND, AEROSOL) AND CHINESE ACDL (AEROSOL, CO2) MISSIONS: VALIDATION AND ALGORITHM REFINEMENT FOR DATA QUALITY IMPROVEMENTS]

<THURSDAY, 14 SEPTEMBER>

ID. 59089

PROJECT TITLE: LIDAR OBSERVATIONS FROM ESA´S AEOLUS (WIND, AEROSOL) AND CHINESE ACDL (AEROSOL, CO2) MISSIONS: VALIDATION AND ALGORITHM REFINEMENT FOR DATA QUALITY IMPROVEMENTS

PRINCIPAL INVESTIGATORS: China Prof. Songhua Wu[1], Europe Dr. Oliver Reitebuch[2]

CO-AUTHORS: Weibiao Chen[3], Xingying Zhang[4], Guangyao Dai[1], Kangwen Sun[1], Xiaoying Liu[1], Oliver Lux[2], Xiaochun Zhai[4]

1 Ocean University of China (OUC), College of Marine Technology, Qingdao, China

2 Deutsches Zentrum f. Luft- u. Raumfahrt (DLR), Institute of Atmospheric Physics, Wessling, Germany

3 Shanghai Institute of Optics and Fine Mechanics (SIOM), Chinese Academy of Sciences, Shanghai, China

4 China Meteorological Administration (CMA), National Satellite Meteorological Centre (NSMC), Beijing, China

PRESENTED BY: Kangwen Sun

☐Objectives

- **ESA's lidar ALADIN/Aeolus**
  - ➢ Identify and correct the systematic error sources, guarantee and improve the performance of ALADIN (lidar instrument installed on Aeolus) and the data quality of the wind products
  - ➢ Explore the scientific application of Aeolus products
- **Chinese lidar ACDL/DQ-1**
  - ➢ Establish and refine the aerosol and cloud optical properties retrieval algorithm of high spectral resolution lidar channel

☐Topics

- **ESA's lidar ALADIN/Aeolus**
  - ➢ Calibration
  - ➢ Validation of wind products
  - ➢ Scientific application of wind and aerosol products
- **Chinese lidar ACDL/DQ-1**
  - ➢ Retrieval algorithm of aerosol and cloud optical properties

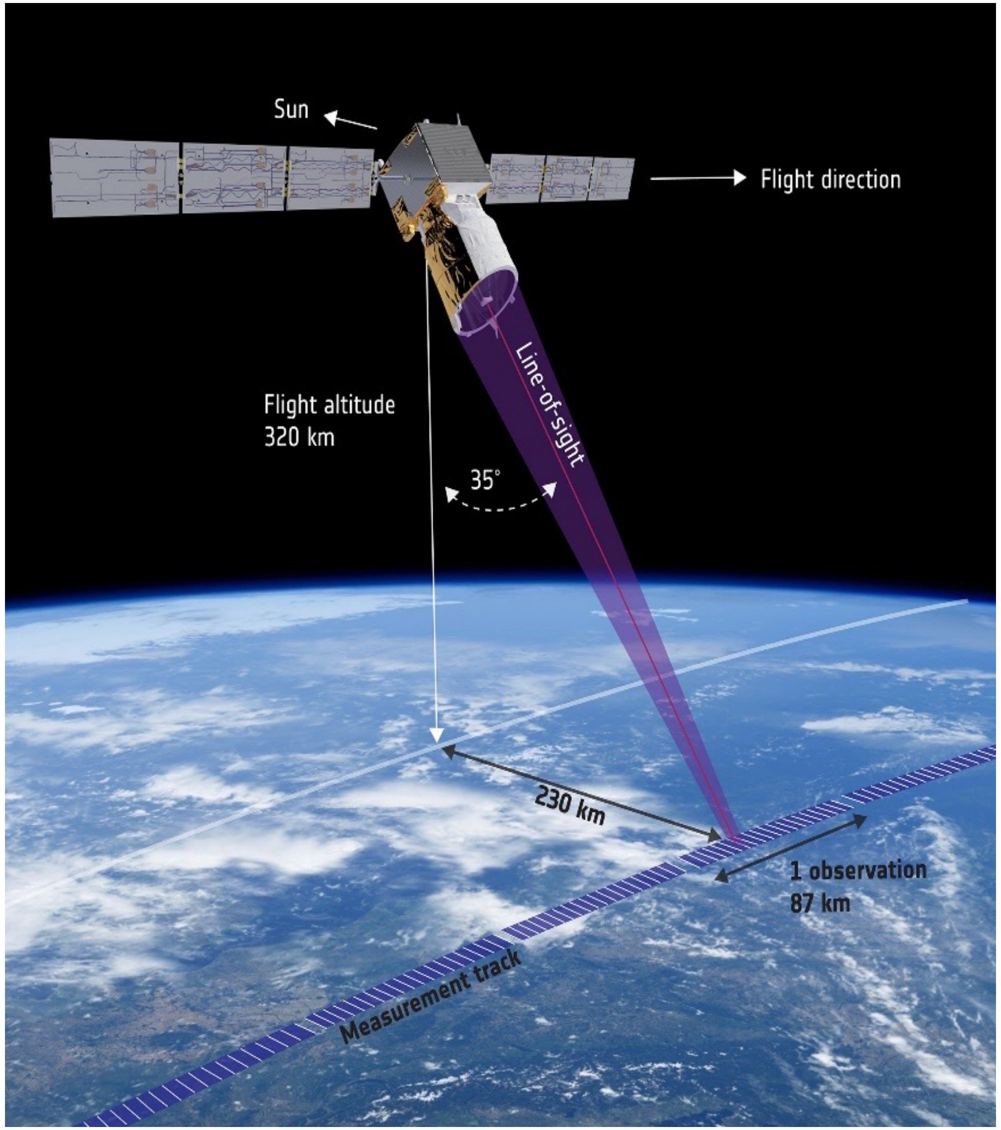

ALADIN on Aeolus:

- the worldwide first wind profile lidar
- launched on 22 August 2018
- retired on 30 April 2023

Product level	Data
L2A	Particle optical properties profiles: ➢ extinction coefficient ➢ backscatter coefficient
L2B	wind profiles: ➢ horizontal line of sight (HLOS) wind
L2C	wind profiles: ➢ reanalysis wind vector assimilated with L2B HLOS wind

Calibration of ALADIN: ALADIN laser frequency stability and its impact on wind measurement

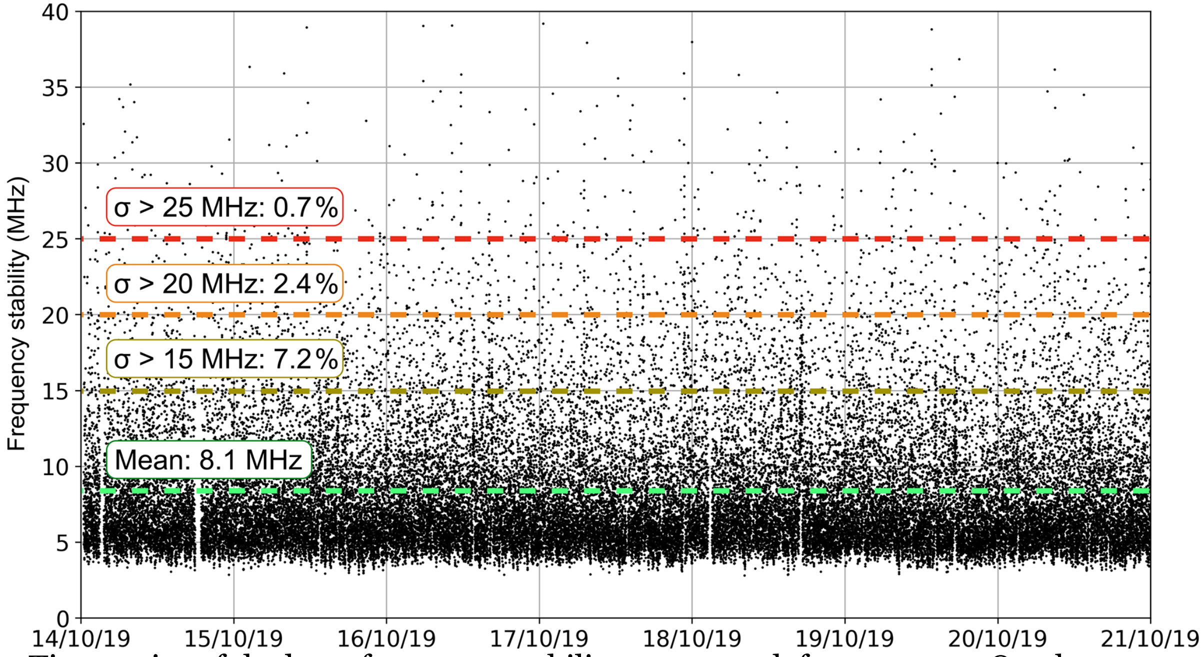

Time series of the laser frequency stability over 1 week from 14 to 21 October 2019

Monitoring the ALADIN laser frequency over more than 2 years :

- excellent frequency stability with pluse-to-pluse variations of about 10MHz
- the permanent occurrence of short periods with significantly enhanced frequency noise (> 30 MHz)

Analysis of the Aeolus wind error with respect to ECMWF model winds:

- frequency stability of the laser has a minor influence on the wind data quality on a global scale
- due to the small percentage of the frequency fluctuations are considerably enhanced

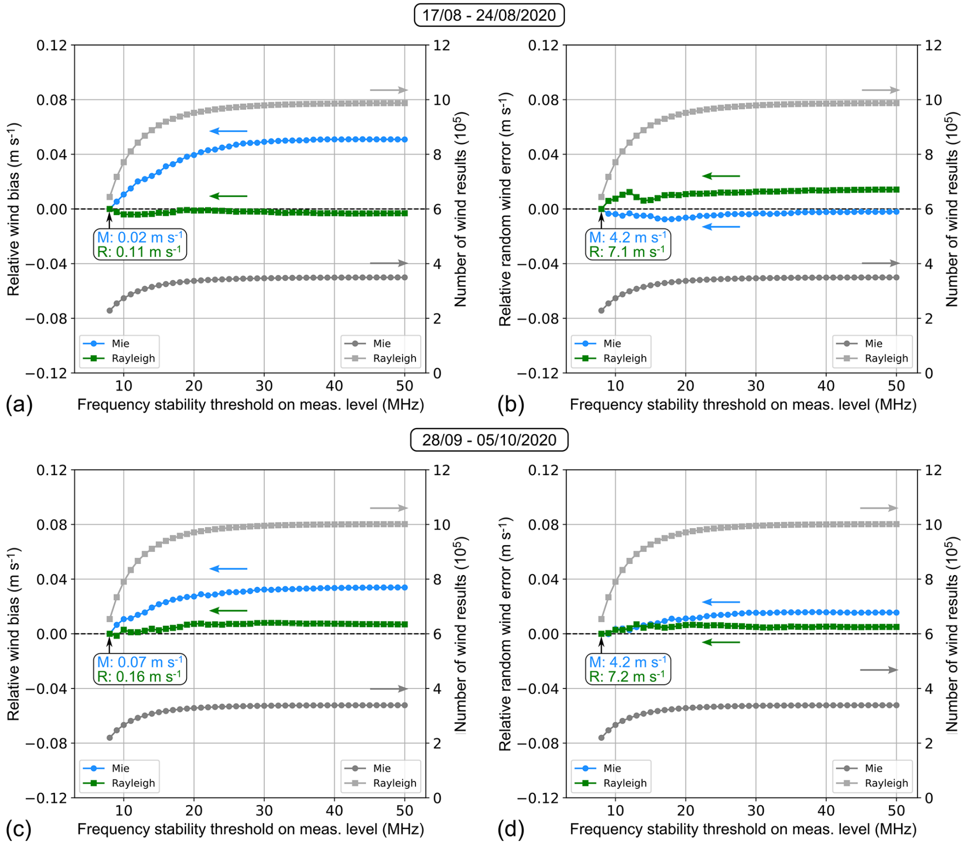

Wind bias (a) and random error (b) of the Mie (blue dots) and the Rayleigh channel (green squares) with respect to the ECMWF model background (O–B) depending on a frequency stability threshold for the period between 17 and 24 August 2020. Panels (c) and (d) show the corresponding data for the week between 28 September and 5 October 2020.

Ref: Lux et al., 2021, AMT.

Calibration of ALADIN: correction of wind bias for ALADIN using M1 telescope temperatures

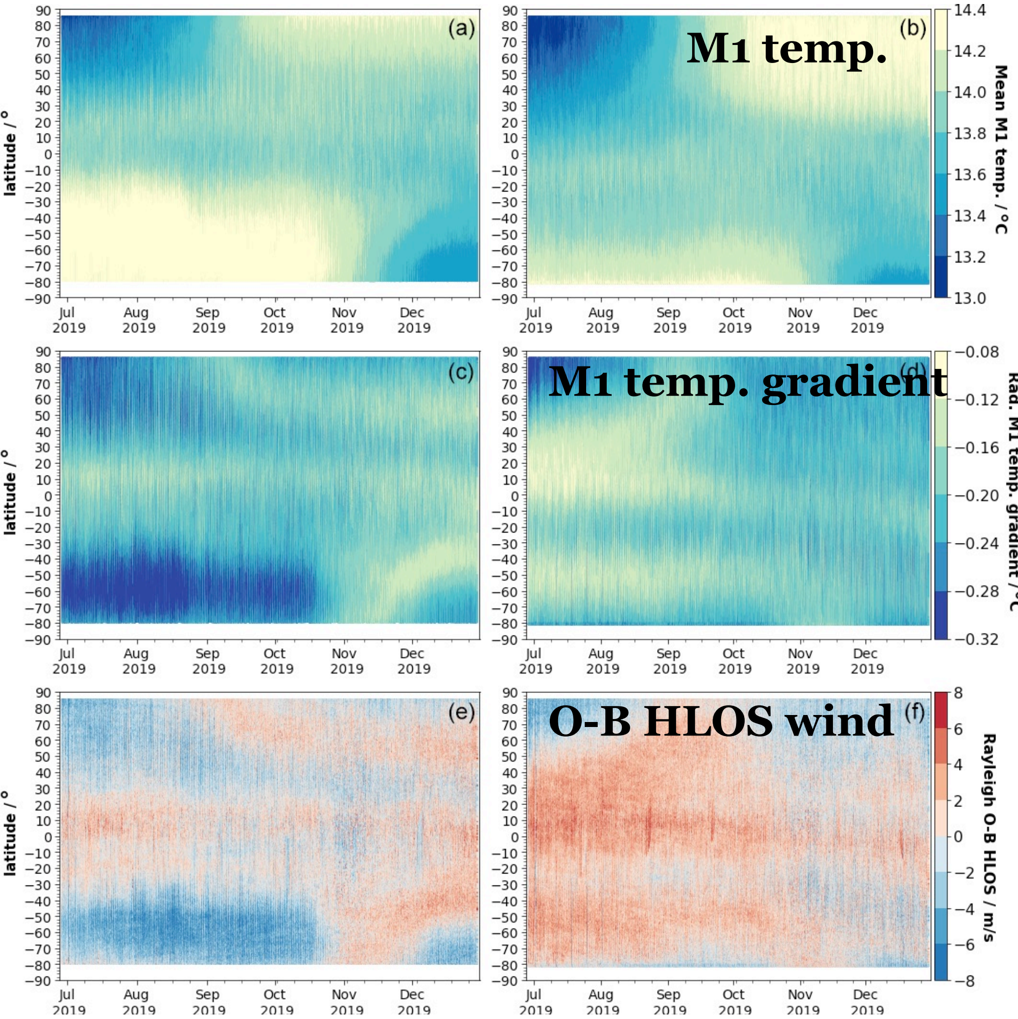

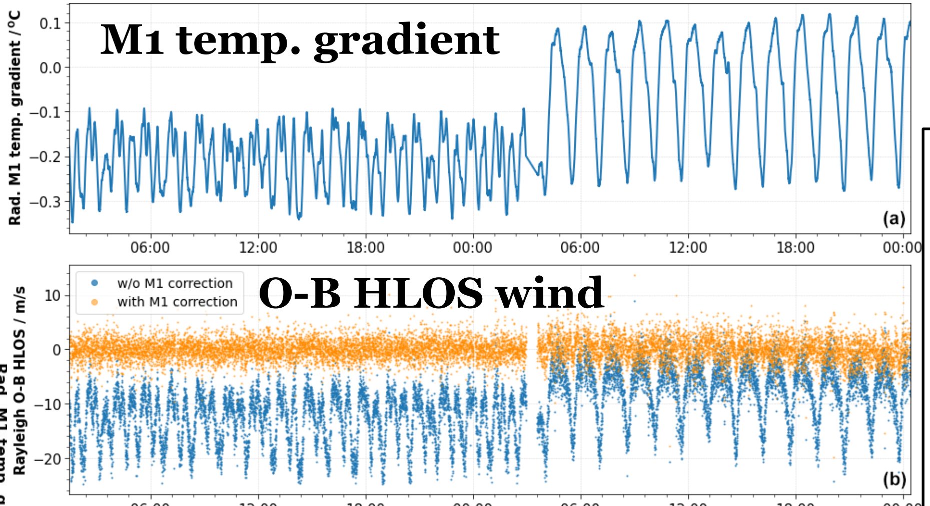

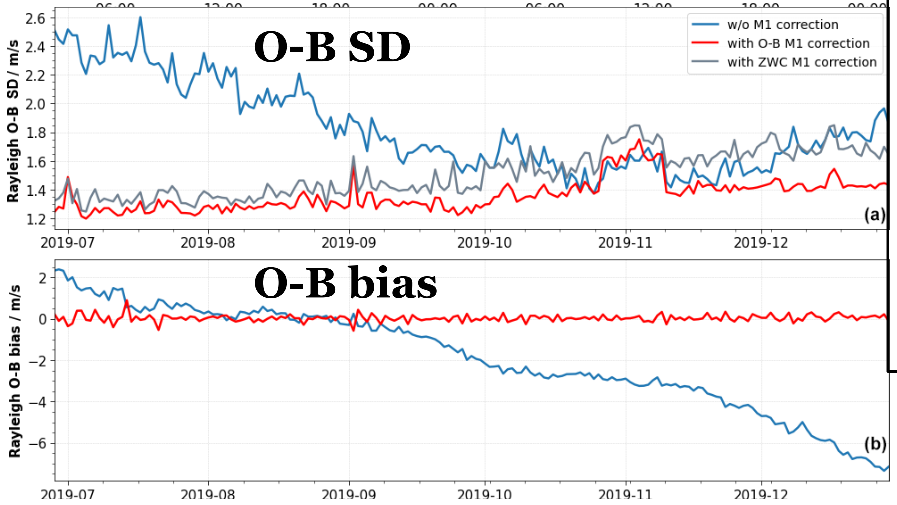

- small fluctuations of the temperatures across the 1.5 m diameter primary mirror of the telescope **cause wind biases of up to 8 m s−1**
- due to changes **in the top-of-atmosphere reflected shortwave and outgoing longwave radiation of the Earth** and the related response of **the telescope's thermal control system**
- ✓ **ECMWF model-equivalent winds** are used as a reference to describe the wind bias **to correct for this effect**

Ref: Weiler et al., 2021, AMT.

Validation of ALADIN: validation with co-located airborne wind lidar A2D observations

Flight no.	Date	Flight period (UTC)	Measurement period (UTC)	No. of A2D observations	Geolocation of DLR Falcon on Aeolus measurement track (start; stop)		No. of Aeolus observations
1	17/11/2018	15:14–19:14	A2D inoperable	No data	44.7° N, 10.6° E;	54.9° N, 7.8° E	12
2	**22/11/2018**	**14:29–17:56**	15:11–15:48 **16:13–17:15**	122 **176**	46.7° N, 16.8° E; **40.5° N, 18.1° E;**	42.3° N, 17.7° E **47.2° N, 16.5° E**	7 **9**
3	29/11/2018	09:56–14:00	Calibration flight				
4	03/12/2018	15:48–19:31	16:48–17:13 17:22–17:48 17:53–18:29	82 87 117	47.8° N, 3.5° E; 50.1° N, 2.9° E; 47.1° E, 3.6° E;	50.5° N, 2.8° E 46.8° N, 3.7° E 50.6° N, 2.7° E	4 4 5
5	05/12/2018	14:56–18:22	15:53–16:45 16:55–17:18	173 78	50.3° N, 18.9° E; 54.0° N, 17.9° E;	54.9° N, 17.6° E 50.8° N, 18.8° E	7 4

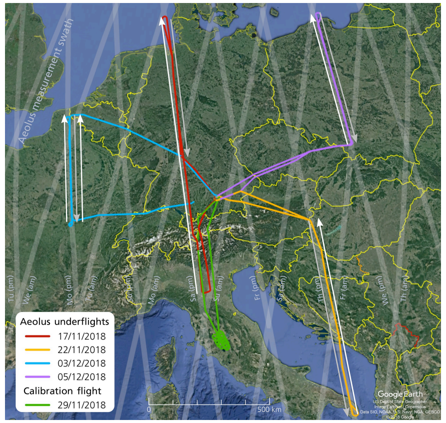

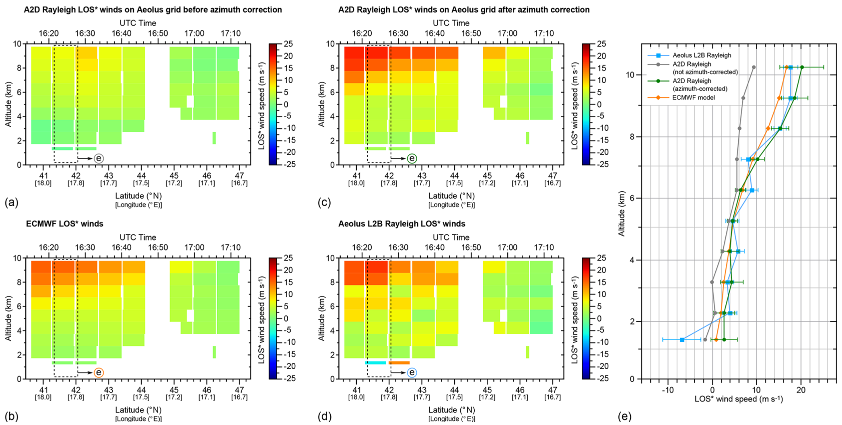

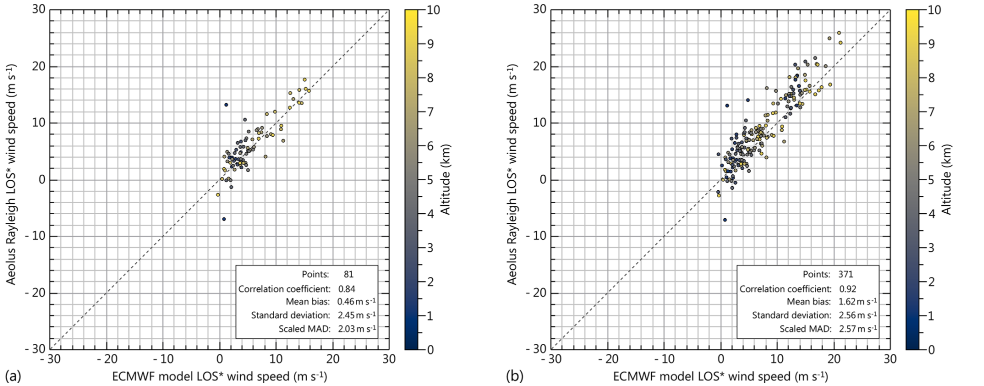

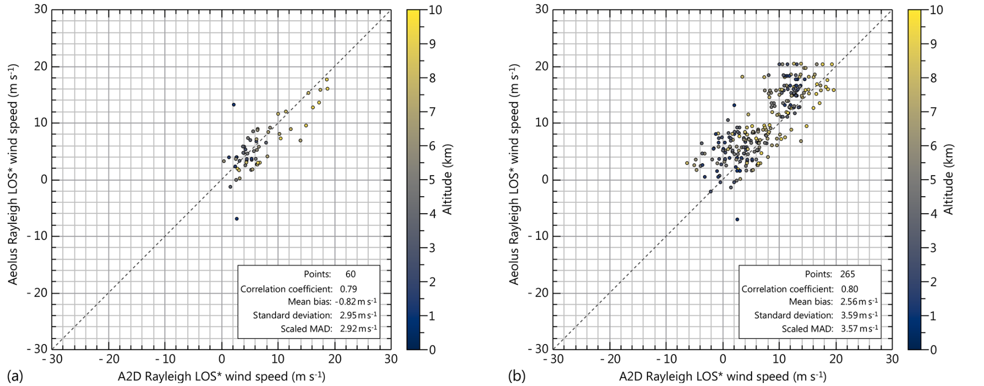

Statistical parameter	A2D Rayleigh vs. 2 µm DWL	A2D Rayleigh vs. ECMWF	Aeolus Rayleigh vs. ECMWF	Aeolus Rayleigh vs. A2D Rayleigh
Number of compared bins	1301	524	371	265
Correlation coefficient (r)	0.83	0.89	0.92	0.80
Slope (A)	0.98 ± 0.02	1.03 ± 0.03	1.08 ± 0.02	0.83 ± 0.04
Intercept (B)	$-0.7\,\mathrm{m\,s^{-1}}$	$-1.2\,\mathrm{m\,s^{-1}}$	$0.9\,\mathrm{m\,s^{-1}}$	$3.8\,\mathrm{m\,s^{-1}}$
Mean bias	$-0.7\,\mathrm{m\,s^{-1}}$	$-0.9\,\mathrm{m\,s^{-1}}$	$1.6\,\mathrm{m\,s^{-1}}$	$2.6\,\mathrm{m\,s^{-1}}$
Standard deviation	$3.7\,\mathrm{m\,s^{-1}}$	$2.6\,\mathrm{m\,s^{-1}}$	$2.6\,\mathrm{m\,s^{-1}}$	$3.6\,\mathrm{m\,s^{-1}}$
Scaled MAD	$3.4\,\mathrm{m\,s^{-1}}$	$2.5\,\mathrm{m\,s^{-1}}$	$2.6\,\mathrm{m\,s^{-1}}$	$3.6\,\mathrm{m\,s^{-1}}$

In the first airborne validation campaign after the launch and still during the commissioning phase of the mission, four coordinated flights along the satellite swath were conducted in late autumn of 2018, yielding wind data in the troposphere with high coverage of the Rayleigh channel.

Ref: Lux et al., 2020, AMT.

Validation of ALADIN: validation with ground-based CDLs over China

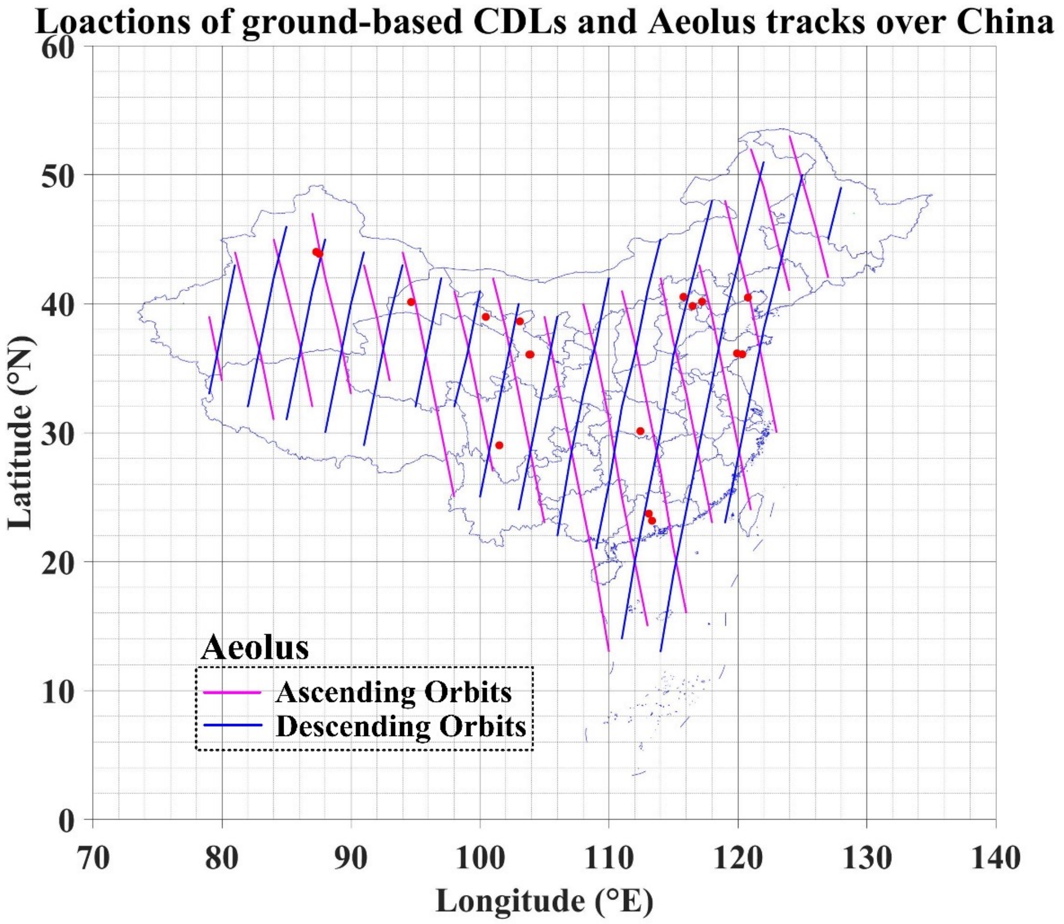

Ground-based CDL observation sites of the VAL-OUC campaign since January 2020

Validation campaigns	Instrument type	Measurement mode	Location	Latitude, longitude, altitude	Measurement period
VAL-OUC	WindMast PBL	DBS*	Dunhuang	40.12° N, 94.66° E; 1.15 km	From 7 Jan to 29 Dec 2020
	WindMast PBL	DBS	Lanzhou	36.05° N, 103.91° E; 1.51 km	From 7 Jan to 29 Dec 2020
	WindMast PBL	DBS	Zhangye	38.97° N, 100.45° E; 1.46 km	From 5 Jan to 27 Dec 2020
	Wind3D 6000	DBS	Jingzhou	30.11° N, 112.44° E; 0.03 km	From 24 Jun to 22 Jul 2020
	Wind3D 6000	DBS	Pinggu, Beijing	40.15° N, 117.22° E; 0.05 km	From 21 Apr to 2 Jun 2020
	Wind3D 6000	DBS	Changji	44.01° N, 87.30° E; 0.58 km	3 Dec 2020
	Wind3D 6000	DBS	Jiulong, Sichuan	29.01° N, 101.50° E; 2.90 km	From 24 Oct to 29 Nov 2020
	Wind3D 6000	DBS	Jiaozhou, Shandong	36.14° N, 119.93° E; 0.02 km	21 Dec 2020
	Wind3D 6000	DBS	Qingyuan, Guangdong	23.71° N, 113.09° E; 0.03 km	From 12 May to 27 Aug 2020
	Wind3D 6000	DBS	Xidazhuangke, Beijing	40.52° N, 115.78° E; 0.91 km	From 7 Jan to 31 Mar 2020
	Wind3D 6000	DBS	Yizhuang, Beijing	39.81° N, 116.48° E; 0.04 km	From 7 Apr to 25 Aug 2020
	Wind3D 6000	DBS	Huludao	40.47° N, 120.78° E; 0.10 km	From 1 Nov to 28 Dec 2020
	Wind3D 6000	DBS	Wuwei	38.62° N, 103.09° E; 1.37 km	From 11 Apr to 26 Dec 2020
	Wind3D 6000	DBS	Lanzhou	36.05° N, 103.83° E; 1.53 km	From 4 Jan to 26 Dec 2020
	Wind3D 6000	DBS	South China University of Technology	23.16° N, 113.34° E; 0.03 km	From 13 Oct to 29 Dec 2020
	Wind3D 6000	DBS	Ürümqi	43.85° N, 87.55° E; 0.84 km	From 14 Oct to 24 Dec 2020
	Wind3D 6000	DBS	Qingdao	36.07° N, 120.34° E; 0.04 km	From 2 Nov to 28 Dec 2020

* DBS: Doppler beam swinging.

Validation of ALADIN: validation with ground-based CDLs over China

CDL introduction and observations over China

Wind3D 6000	
Wavelength	1550 nm
Repetition rate	10 kHz
Pulse energy	150 μJ
Pulse width	100 ns to 400 ns
Detection range	80 m ~ 6000 m (10km extended)
Data update rate	4 Hz (0.25 sec / measurement)
Range resolution	15 m ~ 30 m
Wind speed accuracy	≤ 0.2 m/s
Wind speed range	±75m/s
Wind direction accuracy	0.1°
Power consumption	200W (500W when cooling)
Operating temperature	-30 ~ +50 ℃
Housing classification	IP67
Size	746×764×1000mm
Weight	<80 kg
Data transfer	Ethernet, GPRS (optional)

WindMast PBL	
Wavelength	1550 nm
Repetition rate	10 kHz
Pulse energy	150 μJ
Pulse width	100 ns to 400 ns
Detection range	30 m ~ 4000 m
Data update rate	4 Hz (0.25 sec / measurement)
Range resolution	15 m ~ 30 m
Wind speed accuracy	≤ 0.1 m/s
Wind speed range	±75m/s
Wind direction accuracy	≤ 3°
Operating temperature	-30 ~ +50 ℃
Housing classification	IP65
Size	285×215×430mm
Weight	<30 kg
Data transfer	Ethernet, GPRS (optional)

Validation of ALADIN: validation with ground-based CDLs over China

Intercomparison: Strategy

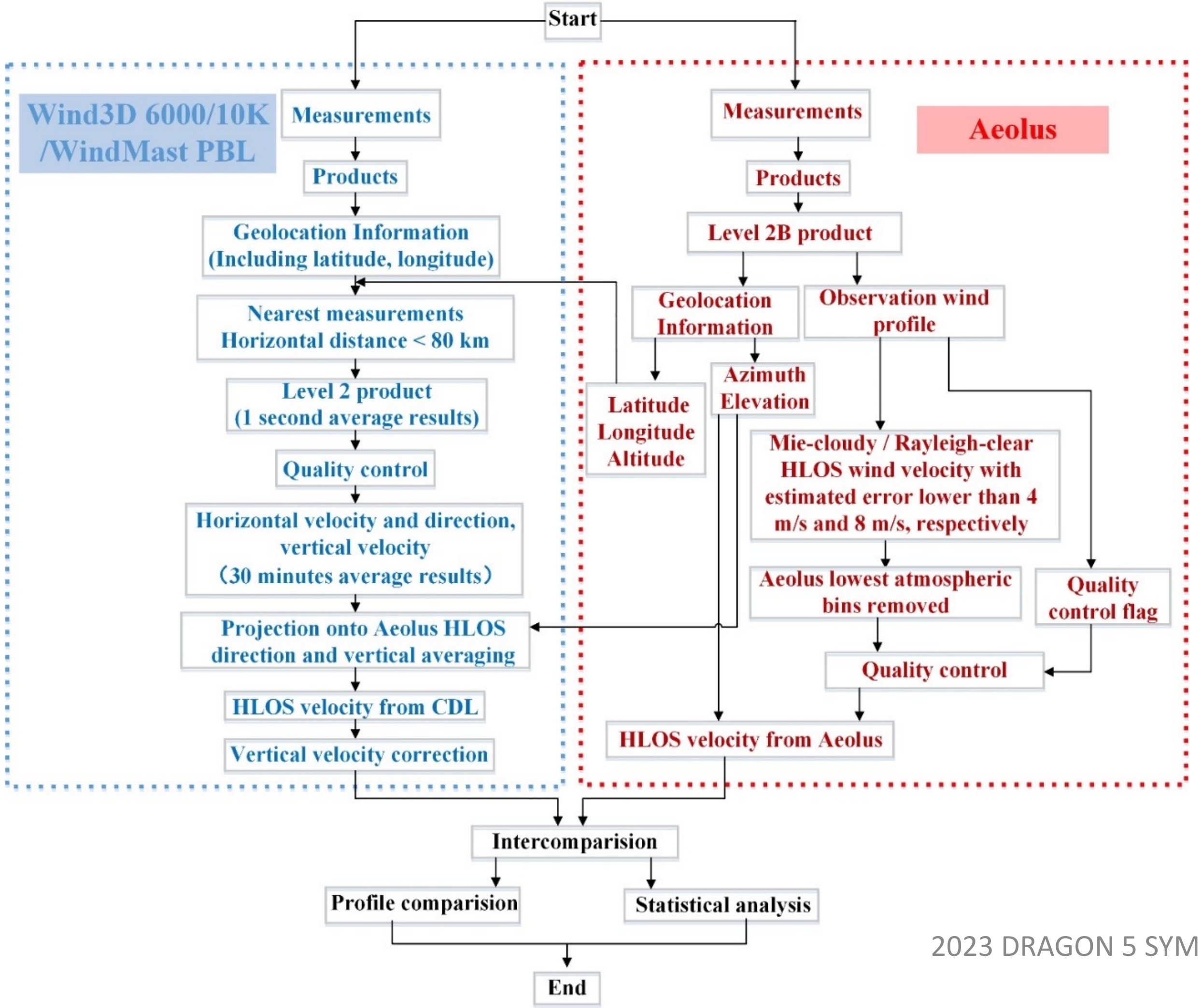

- ➢ Profiles match
- ➢ Quality control
- ➢ Average of CDL wind profiles (time and vertical)
- ➢ CDL wind switching to HLOS wind
- ➢ Profile comparison and statistical analysis

Validation of ALADIN: validation with ground-based CDLs over China

Intercomparison: vertical velocity correction

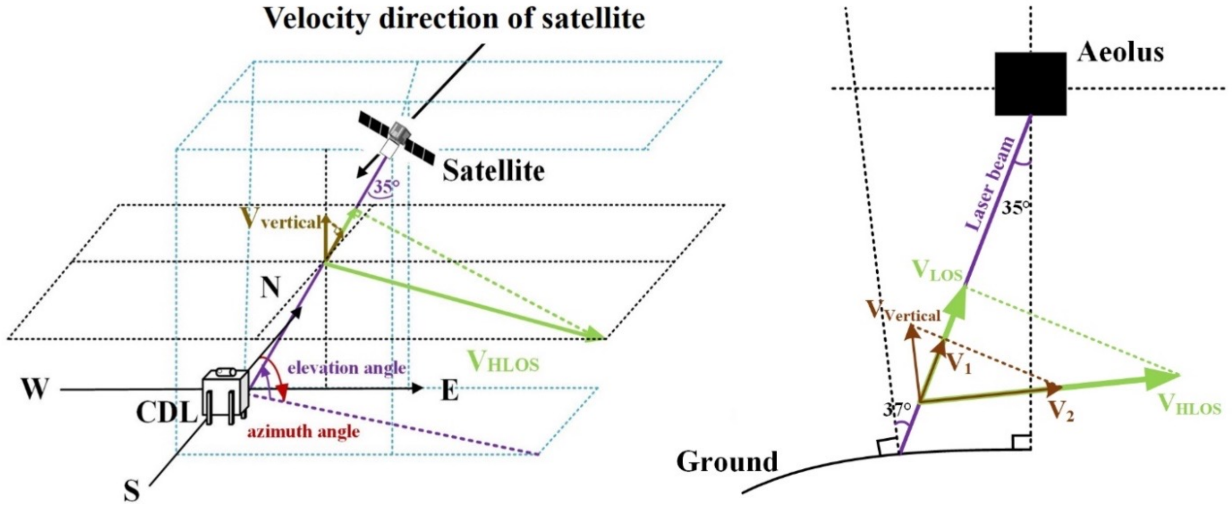

The schematic diagram of the vertical velocity impact on the HLOS velocity retrieval of Aeolus.

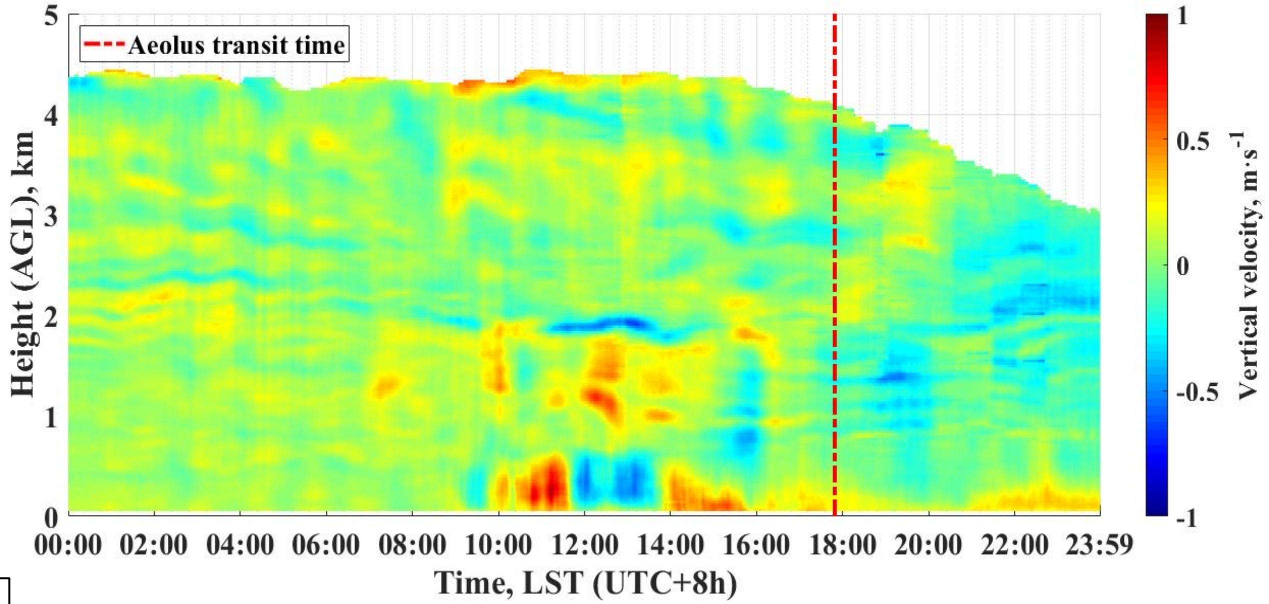

Vertical wind measurement case by CDL with a moving average of 30 minutes, in Qingdao China, on 16 November 2020.

The influence of $V_{vertical}$ on V_{HLOS} is $V_2 = Vvertical \cdot \cos37°/\sin37°$, **i.e.** $V_2 = Vvertical \cdot \cot37°$.

Typical vertical velocity:	HLOS retrieved error:
0 m/s to ±0.40 m/s	**±0.53 m/s**
Max/min vertical velocity: **around 1 m/s / -1 m/s**	**±1.33 m/s**

- In the **atmospheric boundary layers**, where the vertical convections are common, **the influence of vertical velocity on HLOS wind retrieval can not be ignored**.

Validation of ALADIN: validation with ground-based CDLs over China

Results and discussion: measurement cases

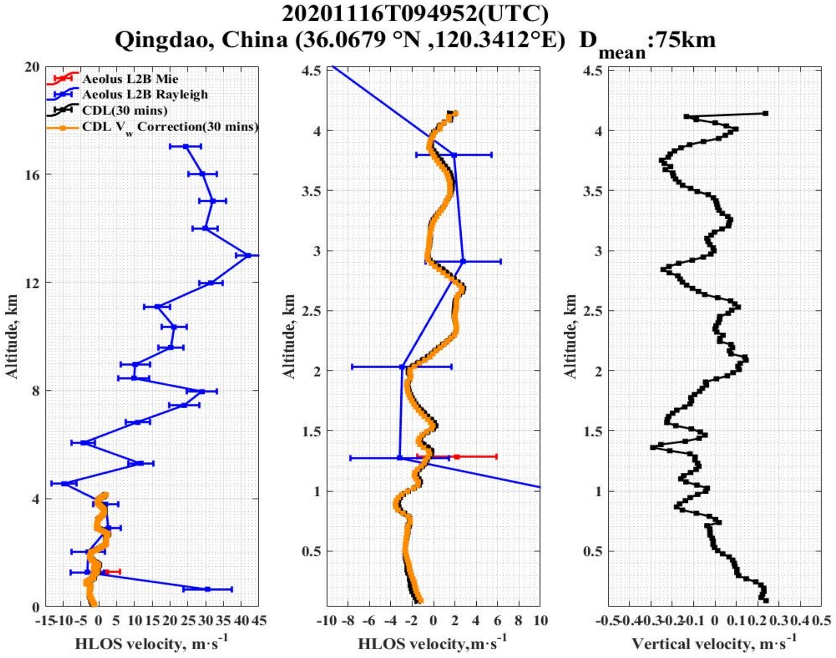

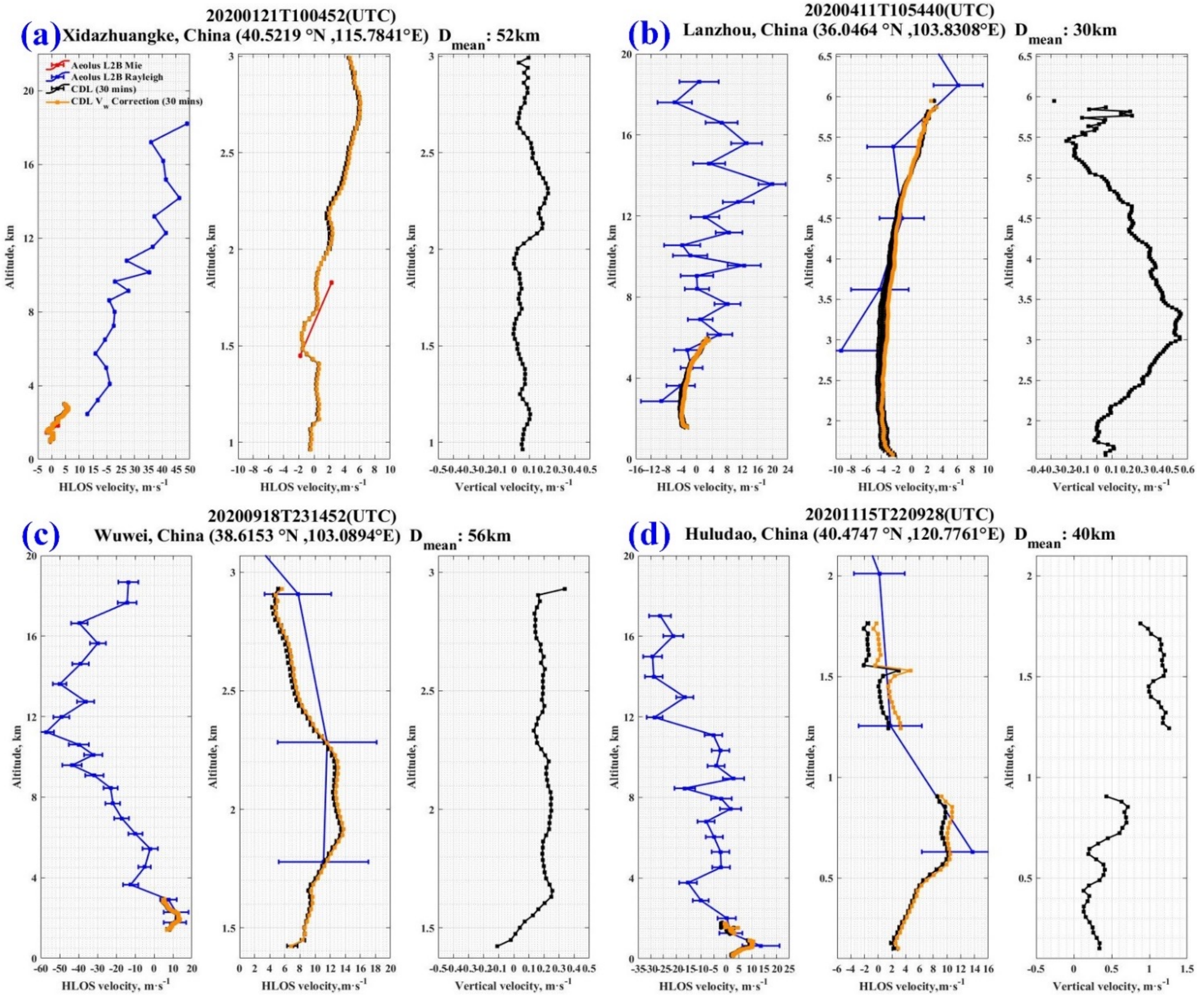

Inter-comparison of HLOS wind velocities measured with CDL and Aeolus on 16 November 2020 at Qingdao (Shandong Province), China:

- **Red lines: Aeolus L2B Mie-cloudy HLOS profiles;**
- **Blue lines: Aeolus L2B Rayleigh-clear HLOS profiles;**
- **Black lines: CDL-retrieved HLOS profiles;**
- **Yellow lines: CDL-retrieved HLOS profiles after vertical velocity correction.**

Validation of ALADIN: validation with ground-based CDLs over China

Results and discussion: statistical analysis

We compare the HLOS wind velocity results from Aeolus observations with the accompanying ground-based CDLs measurements within the VAL-OUC campaign.

- the time period of January to December 2020
- 52 simultaneous Mie-cloudy comparison pairs and 387 Rayleigh-clear comparison pairs
- data pairs are mainly in the atmospheric boundry layer and the lower troposphere

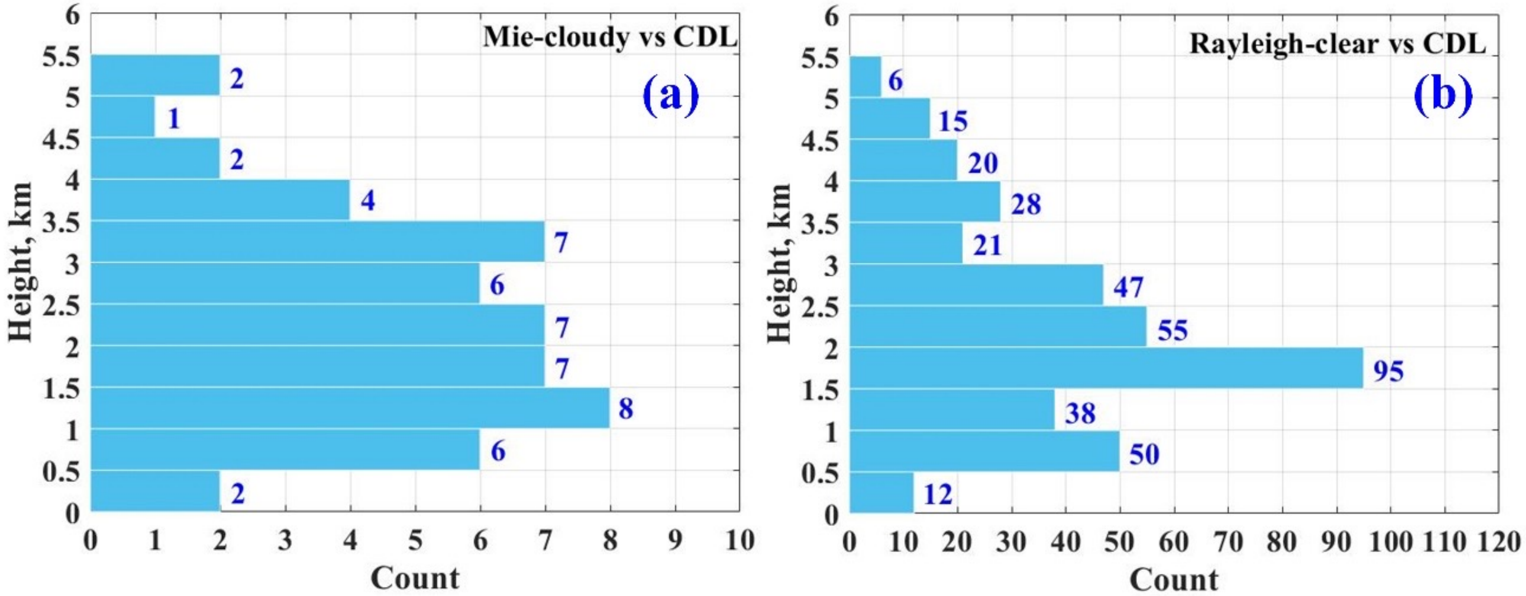

Counts of data pairs at different height ranges of (a) Mie-cloudy vs CDL and (b) Rayleigh-clear vs CDL

Validation of ALADIN: validation with ground-based CDLs over China

Results and discussion: statistical analysis

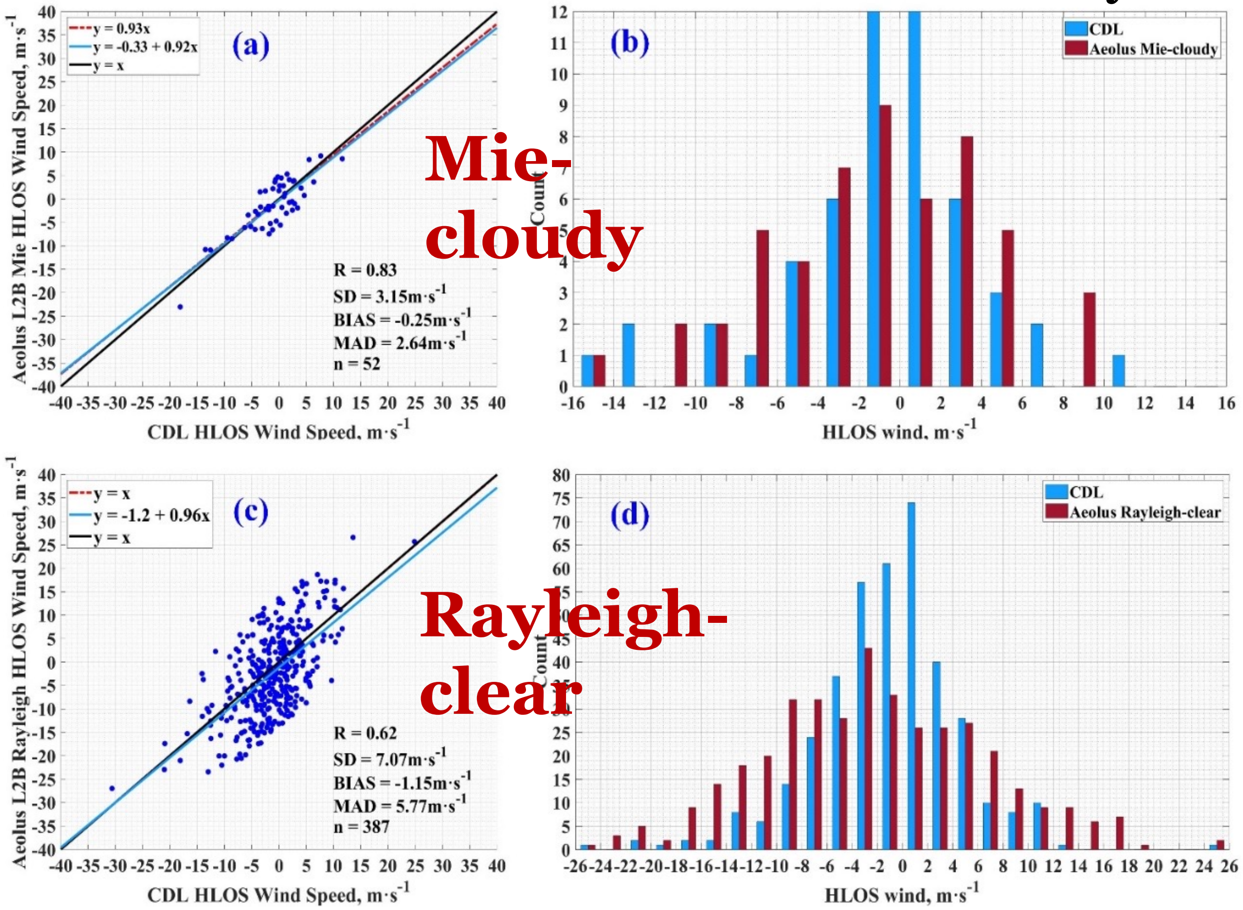

Comparisons of Aeolus L2B Rayleigh-clear HLOS wind velocities and Mie-cloudy HLOS wind velocities against that from CDL.

Statistical comparison of Aeolus HLOS winds and CDL-retrieved HLOS winds

Channel	Mie-cloudy	Rayleigh-clear
N points	52	387
Correlation	0.83	0.62
SD (m/s)	3.15	7.07
Scaled MAD (m/s)	2.64	5.77
BIAS (m/s)	-0.25	-1.15
"y=ax" Slope	0.93	1.00
"y=ax+b" Slope	0.92	0.96
"y=ax+b" Intercept (m/s)	-0.33	-1.20

Validation of ALADIN: validation with ground-based CDLs over China

Results and discussion: statistical analysis

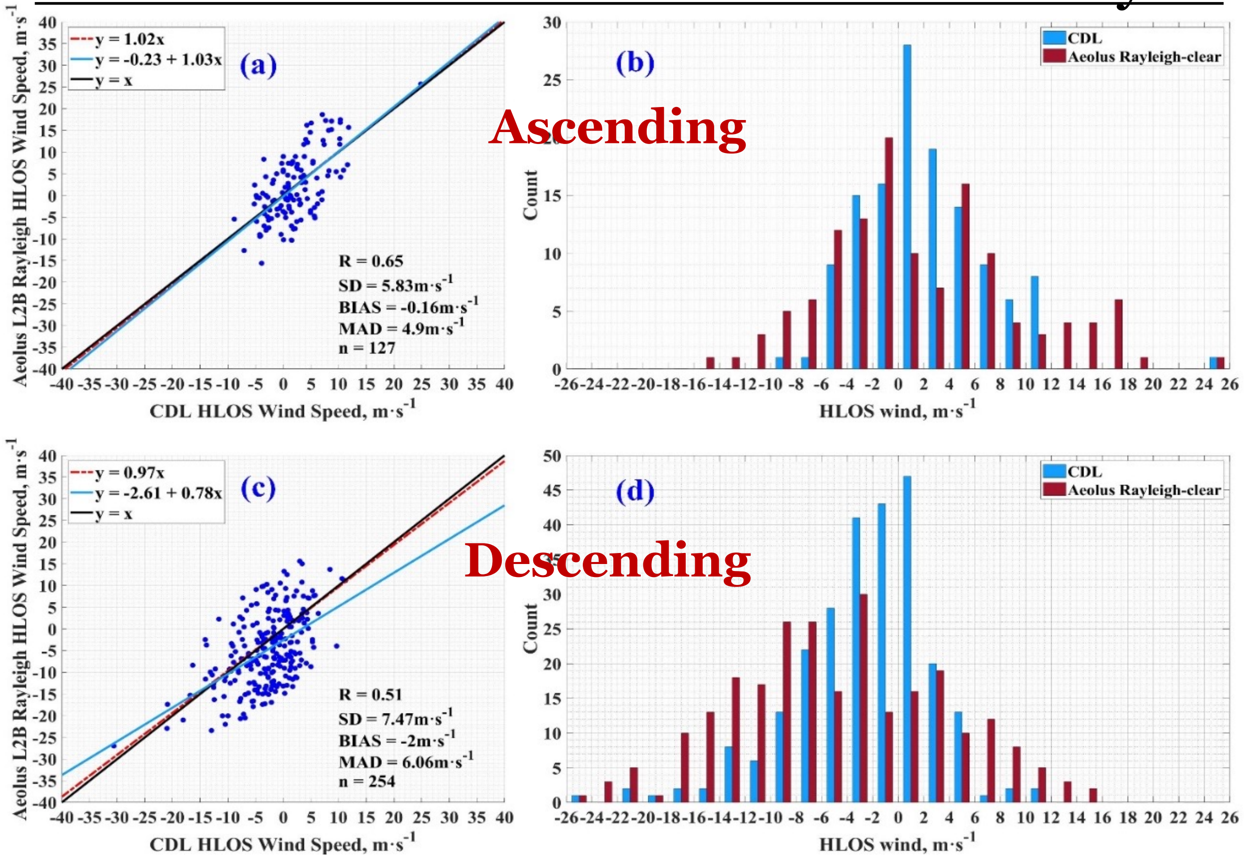

Comparisons of Aeolus Rayleigh-clear HLOS against the CDL-retrieved HLOS according to the measurements made on (a)(b) ascending and (c)(d) descending tracks.

Statistical comparison of Aeolus HLOS winds and CDL-retrieved HLOS winds

Ascending/Descending	Ascending	Descending
N points	127	254
Correlation	0.65	0.51
SD (m/s)	5.83	7.47
Scaled MAD (m/s)	4.90	6.06
BIAS (m/s)	-0.16	-2.00
"y=ax" Slope	1.02	0.97
"y=ax+b" Slope	1.03	0.78
"y=ax+b" Intercept (m/s)	-0.23	-2.61

Consequently, the standard deviation, the scaled MAD and the bias on ascending tracks are slightly better than that on descending tracks.

Validation of ALADIN: validation with ground-based CDLs over China

Results and discussion: statistical analysis

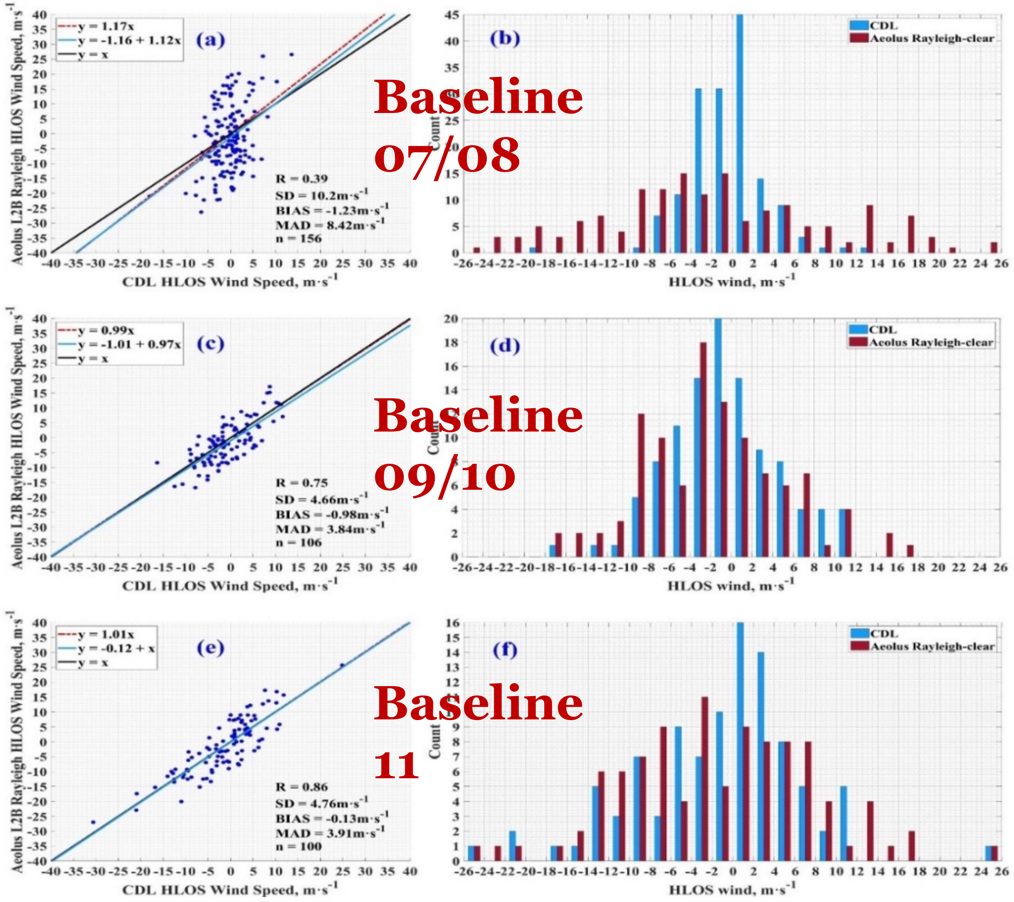

The comparison between the Aeolus L2B Rayleigh HLOS data from (a)(b) Baseline 07 and 08, (c)(d) Baseline 09 and 10, and (e)(f) Baseline 11 against the CDL-retrieved HLOS data.

Statistical comparison of Aeolus HLOS winds and CDL-retrieved HLOS winds

Baselines	07 and 08	09 and 10	11
N points	156	106	100
Correlation	0.39	0.75	0.86
SD (m/s)	10.20	4.66	4.76
Scaled MAD (m/s)	8.42	3.84	3.91
BIAS (m/s)	-1.23	-0.98	-0.13
"y=ax" Slope	1.17	0.99	1.01
"y=ax+b" Slope	1.12	0.97	1.00
"y=ax+b" Intercept (m/s)	-1.16	-1.01	-0.12

Thanks to the

- M1 mirror temperature correction
- different SNR thresholds for classification of Mie and Rayleigh
- Worldwide CAL/VAL team inputs

Baseline 09/10/11 improved significantly than that from Baseline 07/08

Validation of ALADIN: validation with ground-based CDLs over China

Conclusion and outlook

- ✓ The **influence of vertical velocity on V_{HLOS}** in the wind retrieval should be considered.
- ✓ As **the Baseline updating**, the Aeolus L2B HLOS winds (both Mie-cloudy and Rayleigh-clear, mainly in the PBL and the lower troposphere) fitting with the CDL HLOS winds **becomes better**.
- ✓ In the PBL and the lower troposphere, Aeolus **L2B Rayleigh-clear channel** can also provide reasonable HLOS wind.

- ➢ The CDL network in China has been being developed since 2018. The wind profiles from 2018 to 2023 all over China can still be reliable of Aeolus for the validation of FM-A/FM-B/FM-A reprocessing data baselines.

*Ref.: Wu, S., Sun, K., Dai, G., et al., **Inter-comparison of wind measurements in the atmospheric boundary layer and the lower troposphere with Aeolus and a ground-based coherent Doppler lidar network over China**, **AMT**, 2022, Special issue: Aeolus data and their application*

Application of ALADIN: dust transport observation with Aeolus and CALIPSO

Data/models used

Instruments /Models	Products
ALADIN /Aeolus	**L2A (baseline 10)** Particle optical properties: ➢ extinction coefficient@355nm **L2C (baseline 10)** ➢ Reanalysis wind vector profiles assimilated with L2B HLOS wind
CALIOP /CALIPSO	**L2 Aerosol profile** ➢ Extinction coefficient @532nm/1064nm ➢ Backscatter coefficient @ 532nm/1064nm **L2 Vertical Feature Mask** ➢ Aerosol type
ERA5 /ECMWF	0.25°×0.25°, hourly, 37 pressure levels ➢ Wind vector ➢ Relative humidity
The Hybrid Single-Particle Lagrangian Integrated Trajectory (**HYSPLIT**) model	

Application of ALADIN: dust transport observation with Aeolus and CALIPSO

Methodology

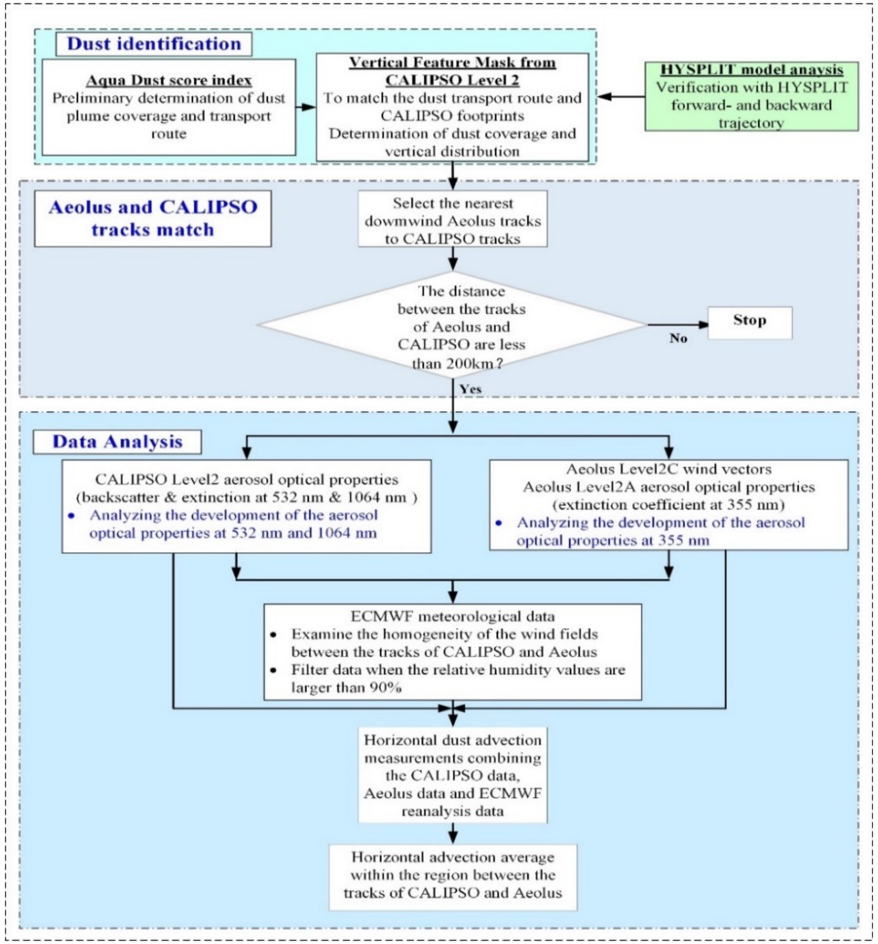

Dust identification, Aeolus and CALIPSO tracks match and data procedures

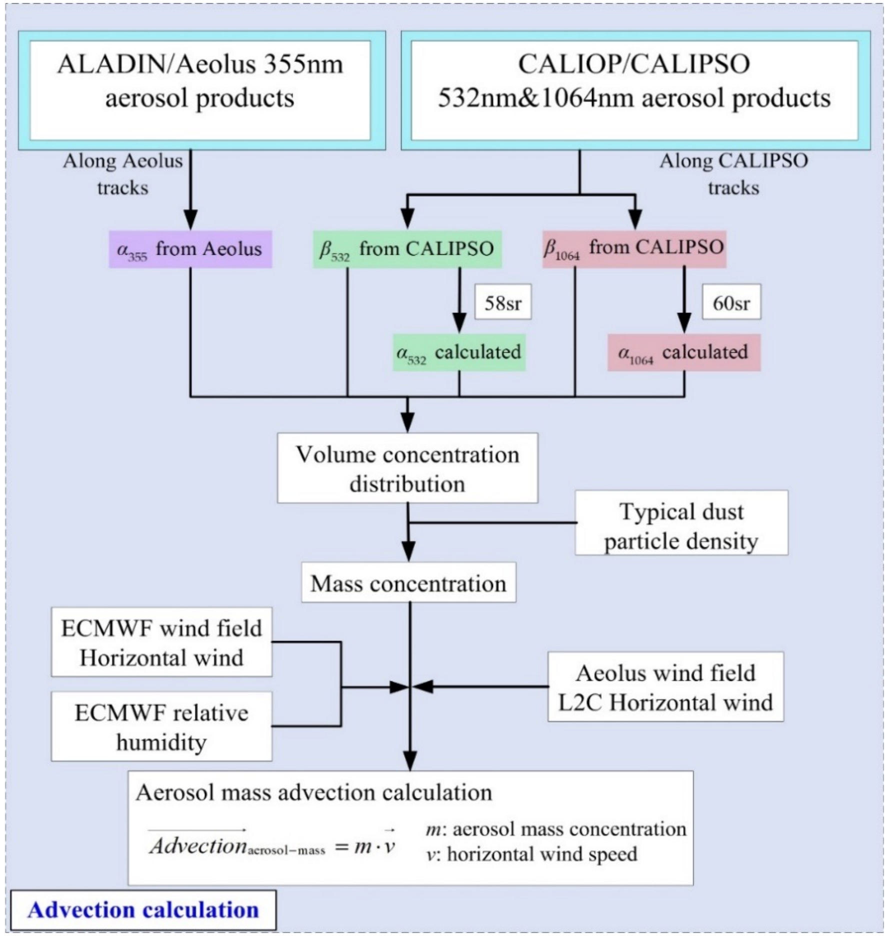

The flowchart of the dust mass advection calculation procedure

Application of ALADIN: dust transport observation with Aeolus and CALIPSO

Results and discussion

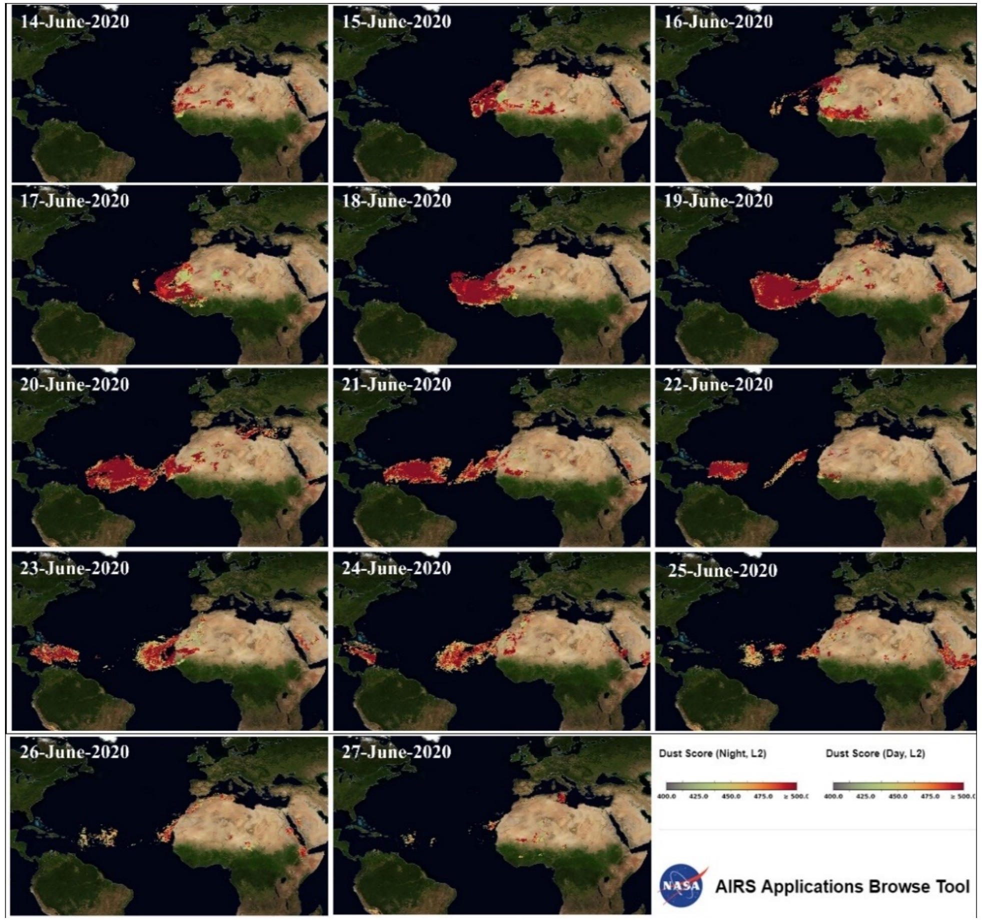

The Dust Score Index provided by AIRS/Aqua at different stages, including emission, transportation, dispersion and deposition

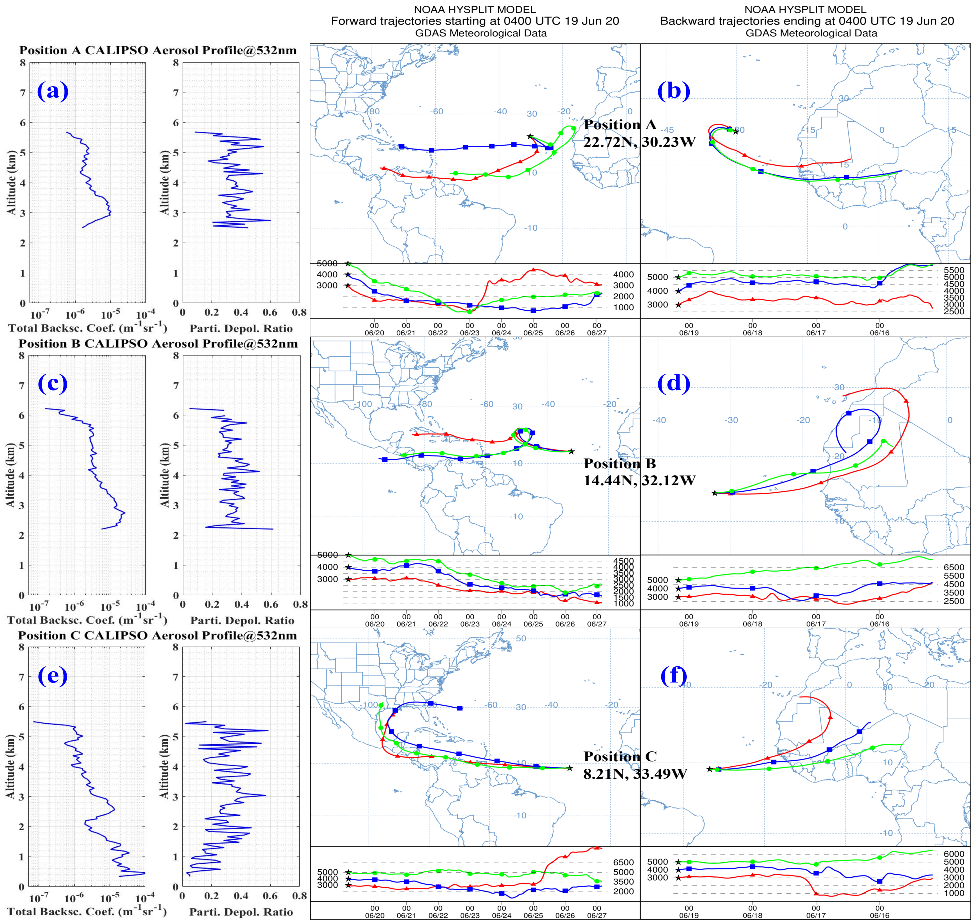

(a)(c)(e) CALIPSO total backscatter coefficient profiles and particle depolarization ratio profiles capturing dust layers at around 0400UTC 19 June 2020. (b)(d)(f) HYSPLIT backward trajectories and forward trajectories at different positions of corresponding CALIPSO profiles and different altitudes on 0400UTC 19 June 2020.

Application of ALADIN: dust transport observation with Aeolus and CALIPSO

Results and discussion: Measurement case

Cross-section	1	2	3
Mean mass concentration, mg/m³ (the retrieval method)	0.28±0.23	0.26±0.24	0.22±0.19
Mean mass concentration, mg/m³ (the factor method)	0.37±0.24	0.40±0.25	0.39±0.27

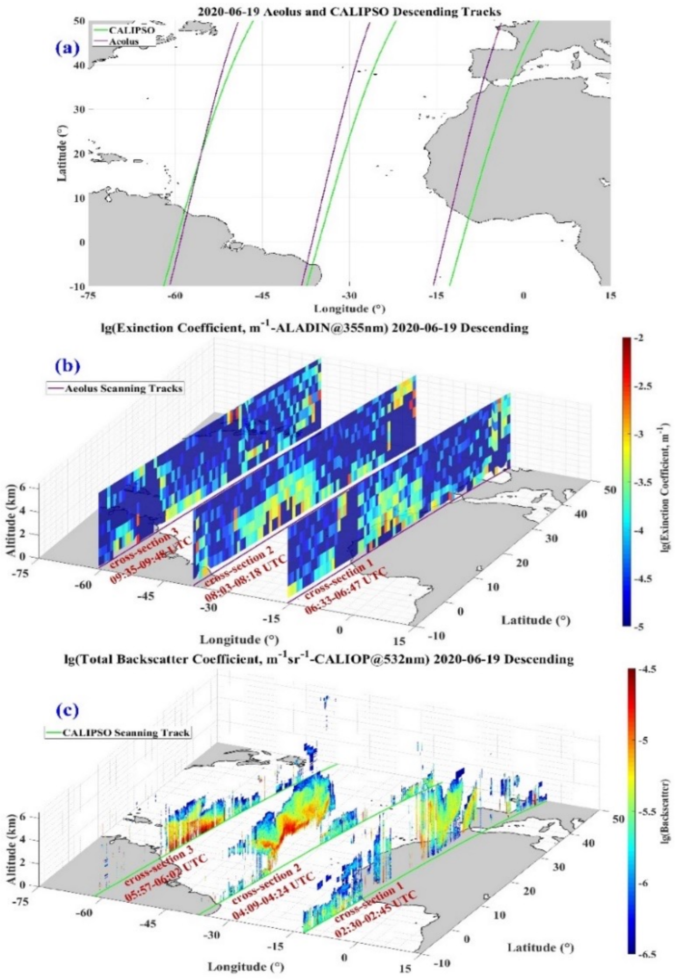

Observation cross-sections of Aeolus and CALIPSO on 19 June 2020

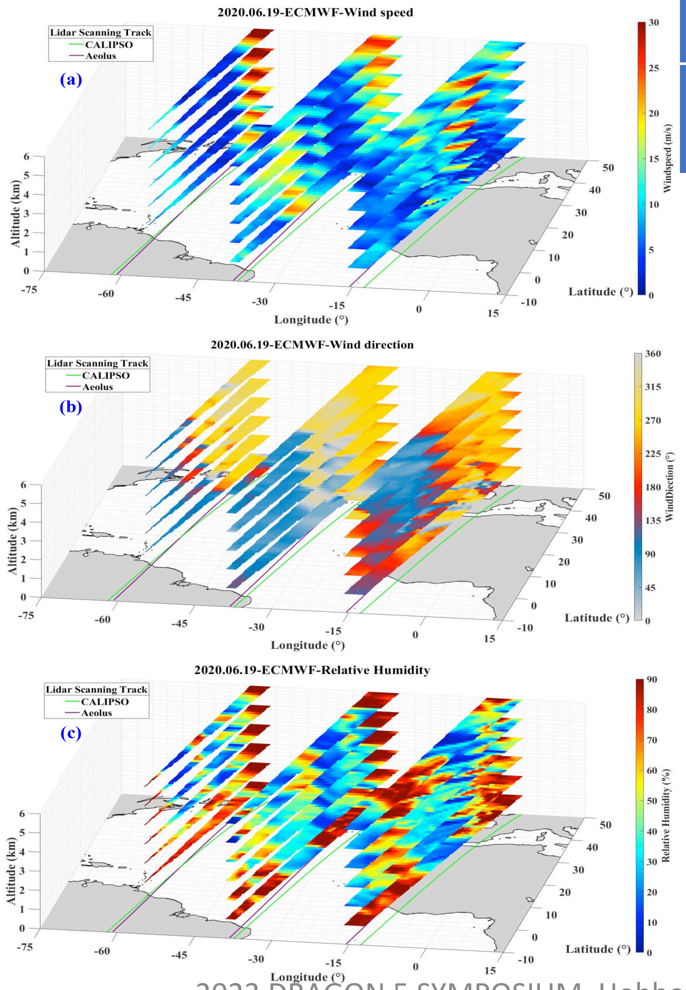

Wind fields and RH from ECMWF

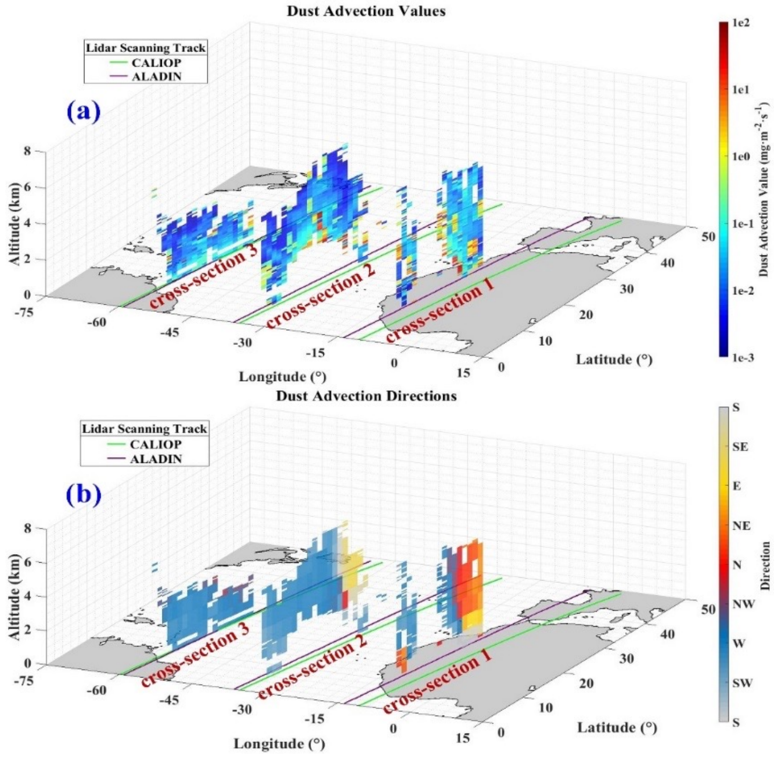

The dust advection calculated with data from ALADIN, CALIOP and ECMWF

Application of ALADIN: dust transport observation with Aeolus and CALIPSO

Results and discussion: dust lifetime

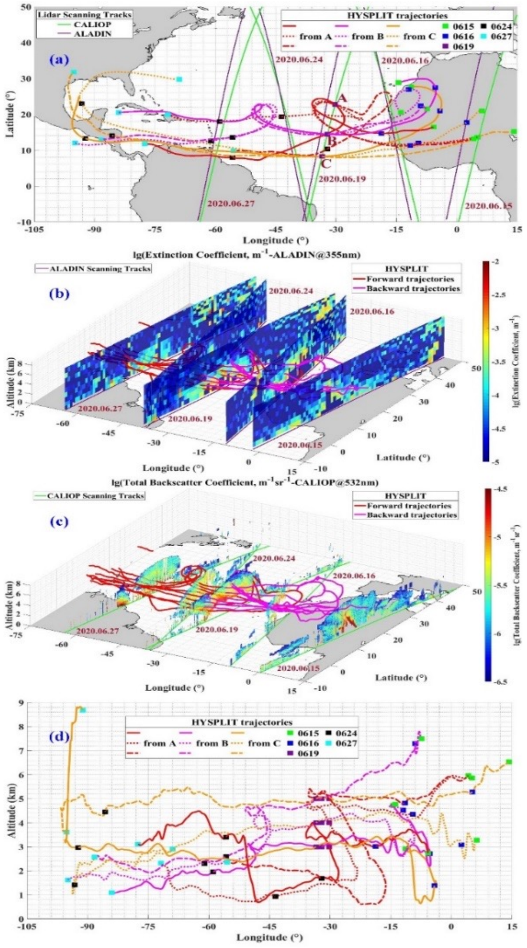

Observation of dust event during 15 and 27 June 2020 with ALADIN and CALIOP and the corresponding HYSPLIT trajectories

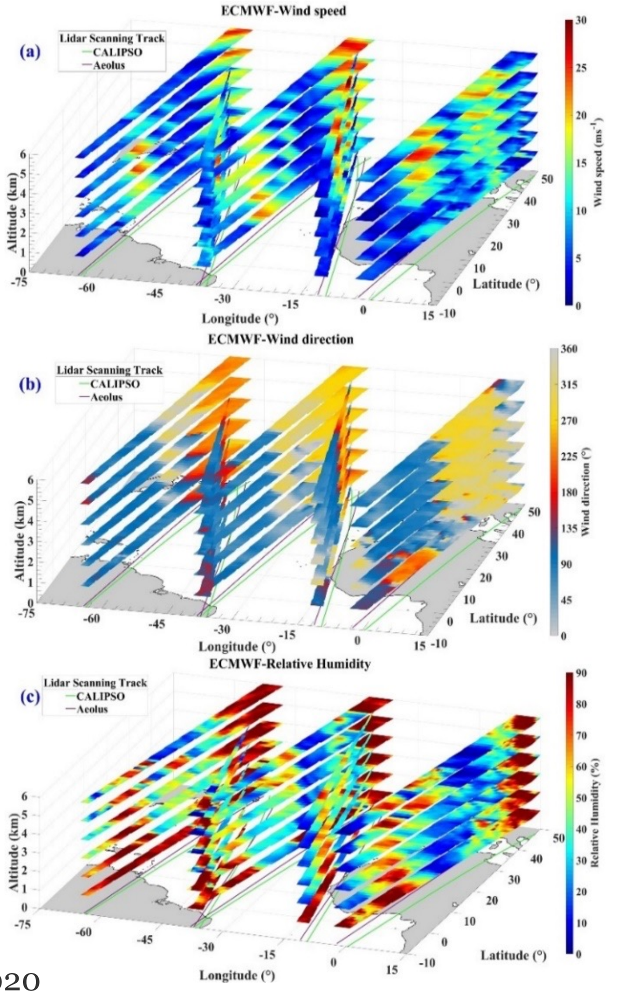

Wind fields and RH from ECMWF

Date	15 June	16 June	19 June	24 June	27 June
Mean mass concentration, (mg/m³,the retrieval method)	0.30±0.23	0.27±0.24	0.26±0.24	0.27±0.24	0.22±0.19
Mean mass concentration, mg/m³ (the factor method)	0.26±0.17	0.39±0.24	0.40±0.25	0.42±0.21	0.34±0.20

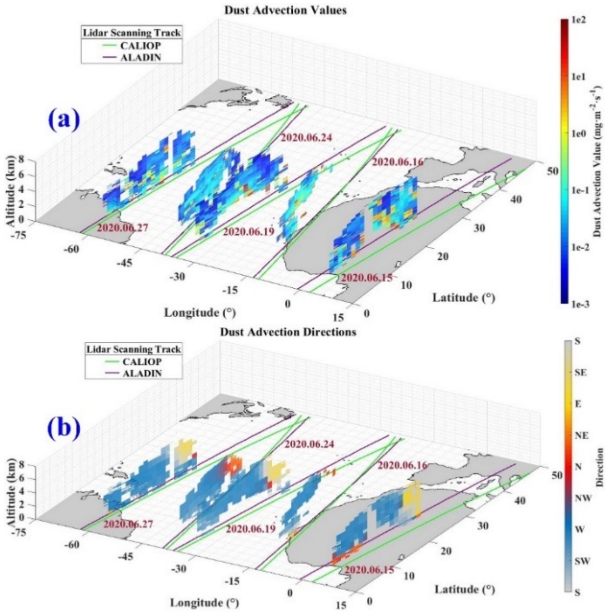

The dust advection

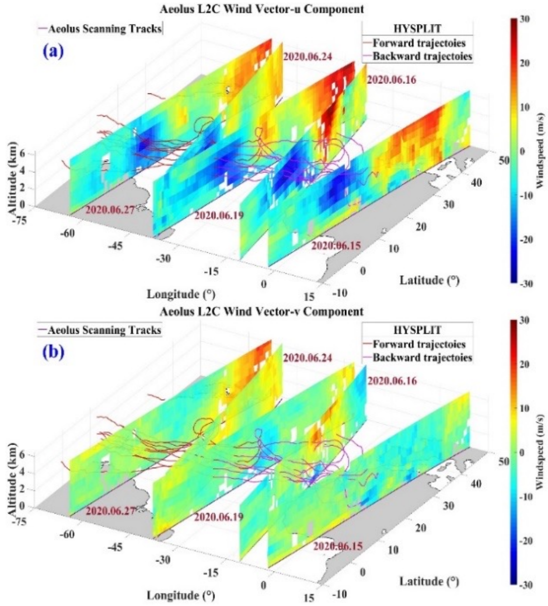

The u and v components

Application of ALADIN: dust transport observation with Aeolus and CALIPSO

Summary and Conclusion

- ✓ ALADIN has the ability
  - on the observations of dust optical properties and wind fields
  - on **tracking the dust events**
  - **calculating the dust mass advection** with the combination of satellite and model data.
- ✓ The huge dust plumes were **trapped and transported in the northeasterly trade-wind zone** between latitudes of 5° and 30° N and altitudes of 0 and 6 km.
- ✓ Aeolus provided the observations of **the dynamics of this dust transport event** in the Saharan Air Layer.

*Ref. : Dai, G., Sun, K., Wang, X., Wu, S. et al., **Dust transport and advection measurement with spaceborne lidars ALADIN and CALIOP and model reanalysis data**, **ACP**, 2022, Special issue: Aeolus data and their application*

Application of ALADIN: correlation between marine aerosol and wind

Background

Ref. : http://www.oceansinc.org/2013/04/biological-activity-alters-ability-of.html

marine aerosol/sea spray aerosol

- Interaction with solar radiation
- Impact on retrieval of spaceborne ocean color lidar

…

Wind is the primary driver of the emission of marine aerosol

Correlation between **marine aerosol optical properties** and **wind speed**

Data used

Instruments	Products
ALADIN /Aeolus	**L2A (Baseline 11-14)** Particle optical properties: ➢ extinction coefficient ➢ backscatter coefficient NWP: ➢ Relative Humidity (RH) ➢ Molecular backscatter coefficient **L2C (Baseline 09-14)** ➢ Reanalysis wind vector profiles assimilated with L2B HLOS wind
CALIOP /CALIPSO	**L2 Vertical Feature Mask** ➢ Aerosol type

Time range of the data： April 2020 to June 2022

Application of ALAI ct wind

Method

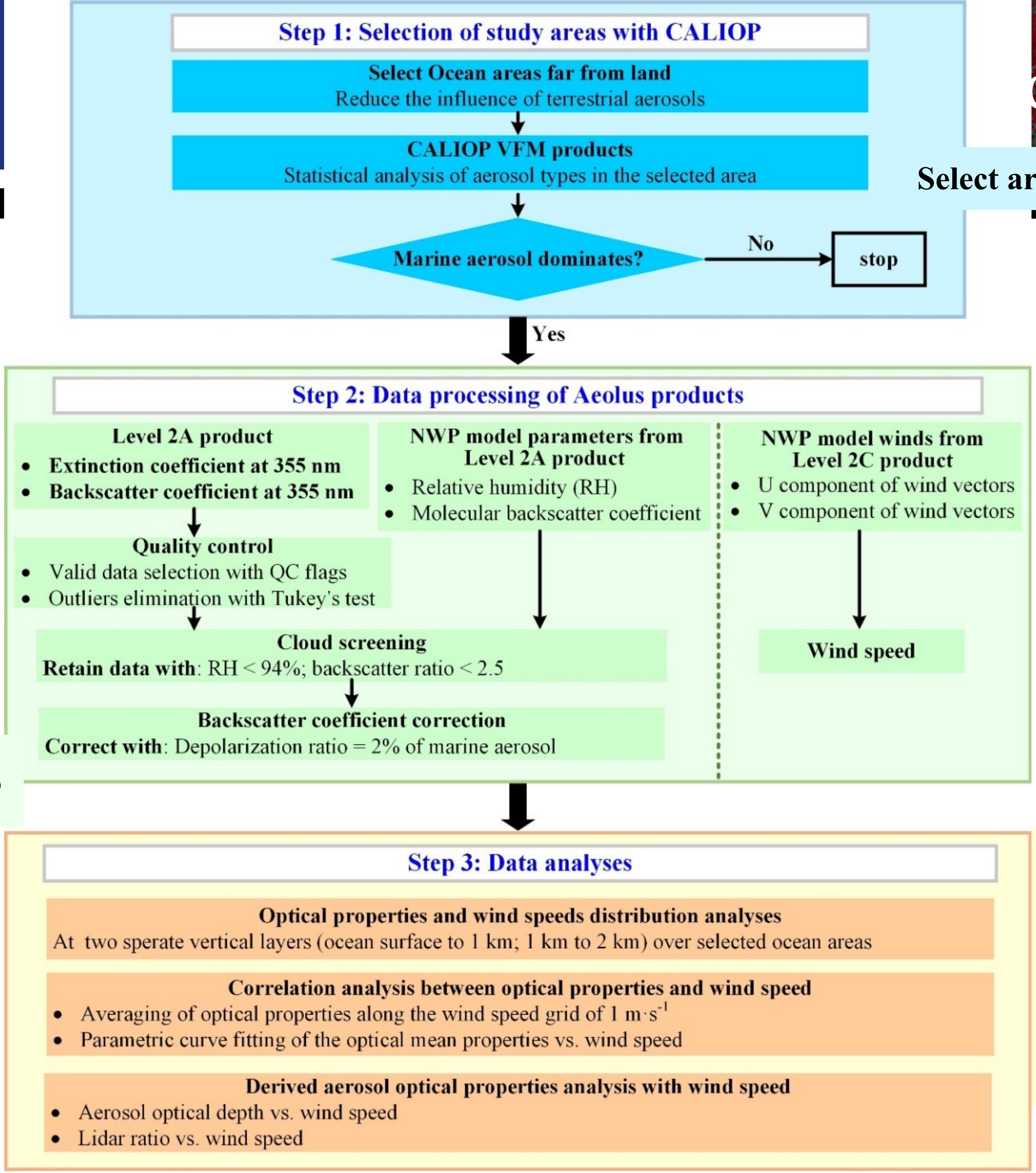

Select areas dominated with marine aerosol

Pure marine aerosol α and β

0-1 km layer ($Layer_L$): corresponding to the marine atmospheric boundary layer (MABL)
1-2 km layer ($Layer_H$): above the MABL
*The lowest bins of L2A products are absent to avoid the ground return signals' contamination

Application of ALADIN: correlation between marine aerosol and wind

Results

Distributions of background wind speed, marine aerosol α, β, lidar ratio at two layers above three study areas

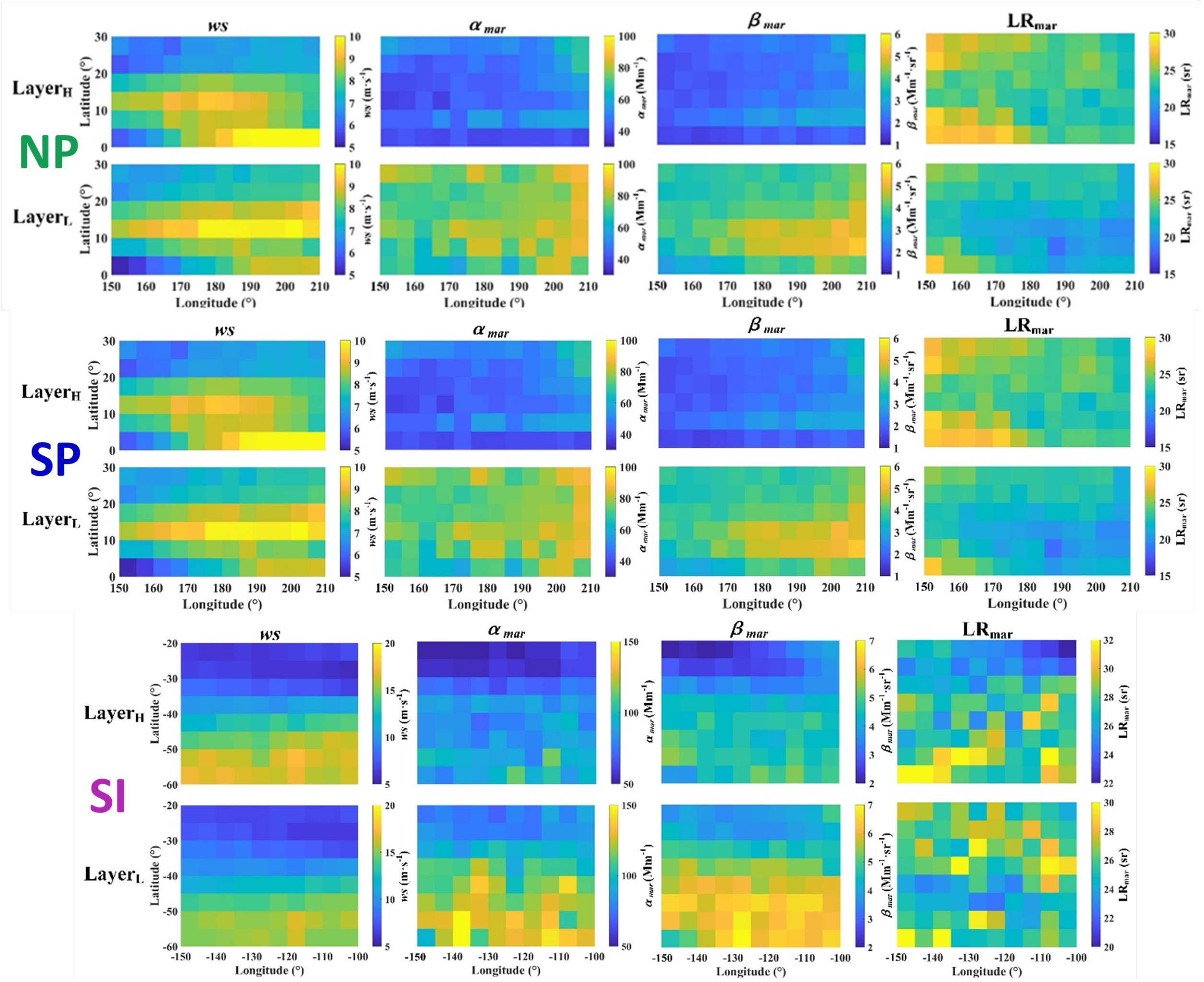

Application of ALADIN: correlation between marine aerosol and wind

Correlations between marine aerosol α, β, lidar ratio vs. wind speed

SP

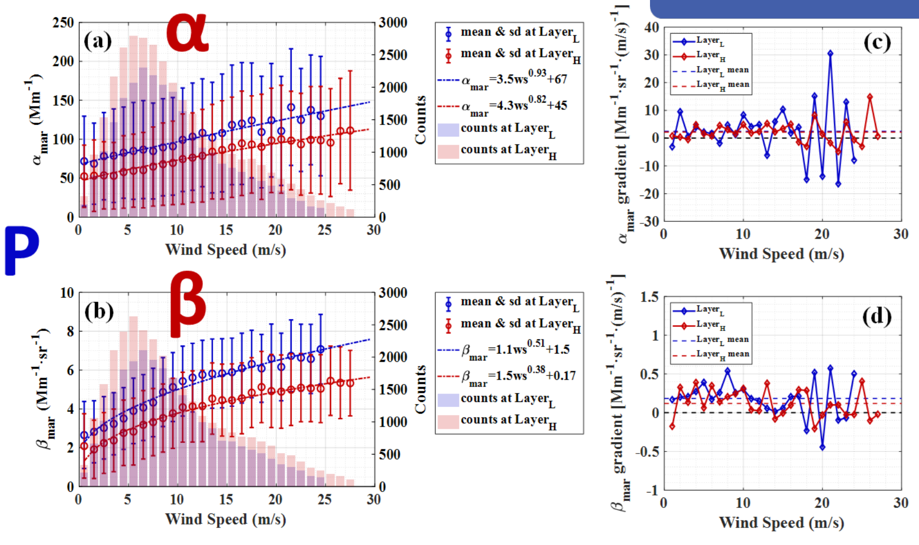

NP

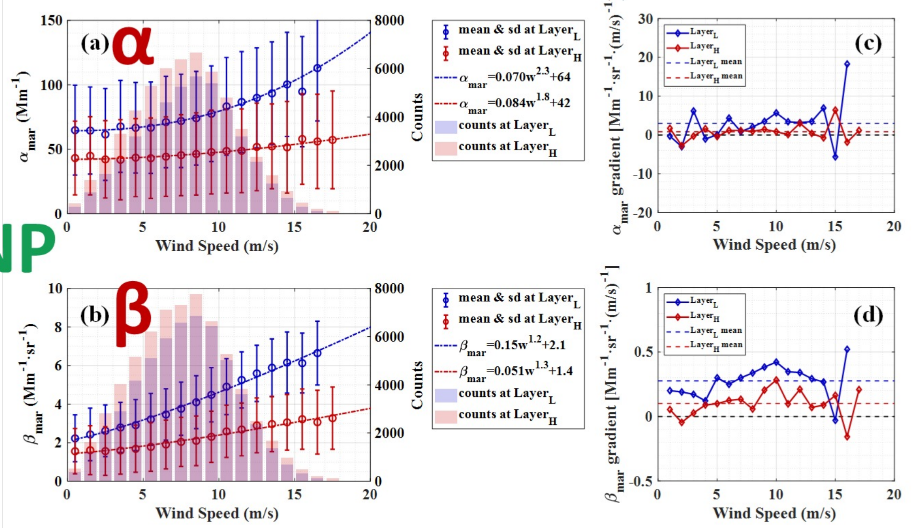

SI

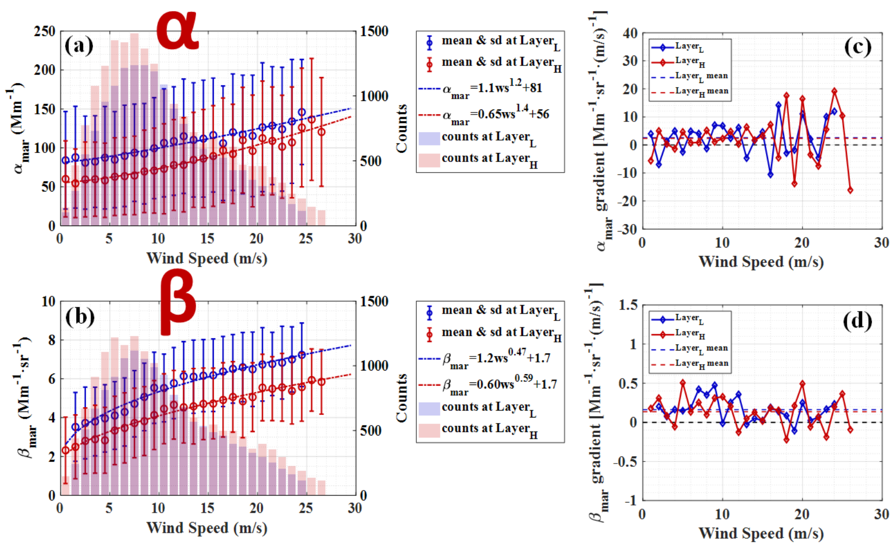

- The marine aerosol extinction/backscatter coefficients and the background wind speeds show positive relationships and they were fitted by **power law functions**, of which the corresponding R^2 are all higher than **0.9**.
- Both the MABL and the higher layer above the MABL will receive the marine aerosol produced and transported by the wind from the air-sea interface.
- The marine aerosol load at the lower layer (MABL) is stronger than at the higher layer. **The marine aerosol enhancements caused by the background wind are more intensive at the MABL.**
- The **gradient change points** of marine aerosol extinction/backscatter coefficients appear during the growth of them with wind speed, above which the growth rate becomes lower. It might illustrate that **the enhancement of marine aerosol driven by wind includes two phases**, among which one is **rapid growth phase** with high dependency of wind, and another is **slower growth phase** after the gradient change points.

Application of ALADIN: correlation between marine aerosol and wind

Results

Correlations between marine aerosol α, β, lidar ratio vs. wind speed

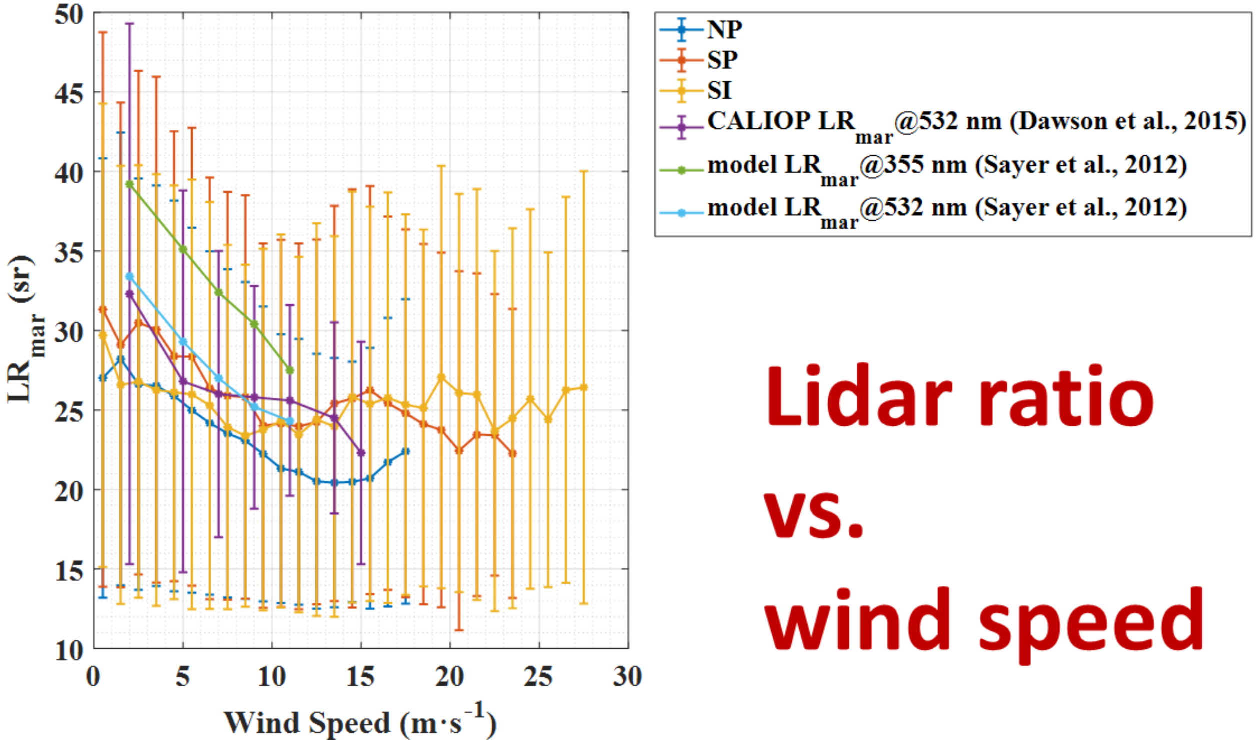

Lidar ratio vs. wind speed

- Marine aerosol lidar ratio and its particle size have **negative relationship**.
- From the analysis from Aeolus data, marine aerosol lidar ratio variation with wind speed shows:
  - **downward trend at low wind speed**, indicating the increasing of particle size;
  - **upward trend at middle wind speed**, indicating the decreasing of particle size.
- The results at low wind speed fit well with previous works.

Application of ALADIN: correlation between marine aerosol and wind

Summary and Conclusion

- ✓ First ever deriving pure **marine aerosol optical properties from Aeolus products**.
- ✓ Acquiring the spatiotemporally synchronous relationship with the aerosol optical properties and the instantaneous wind speeds, which could indicate the **background atmosphere states within and above the MABL over remote ocean**.
- ✓ Conducting analysis at **two separate vertical layers** above ocean surface to explore the vertical differences.

Ref.: Sun, K., Dai, G., Wu, S., et al., ***Correlation between marine aerosol optical properties and wind fields over remote oceans with use of spaceborne lidar observations**,* ***ACPD**, Special issue: Aeolus data and their application*

ACDL/DQ-1: launched on 16 April 2022

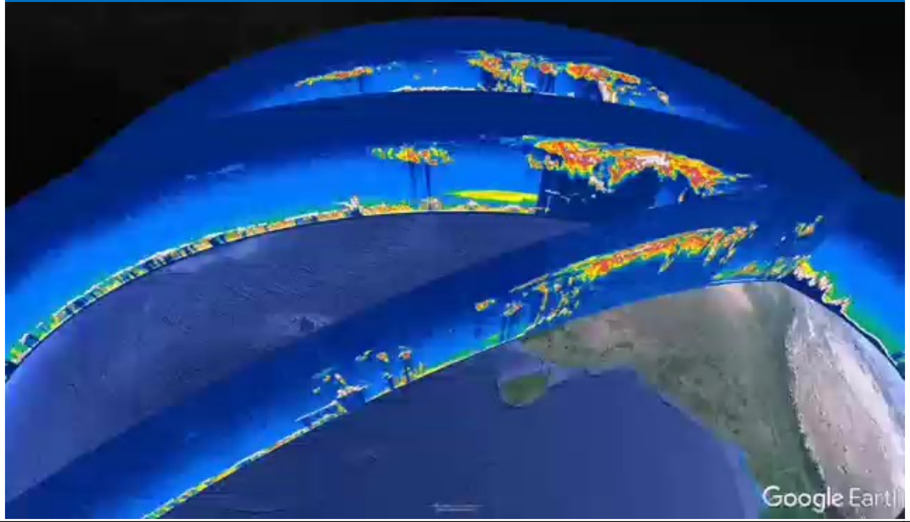

Sensor	Observed object
[main Payload] **Aerosol and Carbon Detection Lidar (ACDL)**	Global column CO_2; Global aerosols and clouds profile; Global pollutant distribution PM2.5 etc.
Particulate Observing Scanning Polarimeter (POSP)	Aerosols and clouds, PM2.5
Directional Polarization Camera (DPC)	Aerosols and clouds, PM2.5
Environmental trace gas Monitoring Instrument (EMI)	NO_2, SO_2, O_3 etc.
Wide Swath Imaging system (WSI)	Temperature and humidity, aerosols and clouds

Specification	Value
Orbit	705 km, sun-synchronous orbit
Revisit duration	~ 51 days
Weight	2.8 t
lifetime	＞ 8 years

Chinese lidar ACDL/DQ-1: retrieval algorithm

level	Data processing	Data products	Format
Level 0	The observation data obtained by downlinking multi-packet data integrity inspection and data splicing through the two channels of the satellite.	Raw data	RAW
Level 1A	Process the level 0 aerosol data, obtain the profiles of 532 nm and 1064 nm channels, with the geographic location and height corrected.	Profiles data of 532 nm and 1064 nm channels	HDF5
Level 1B	Process the level 0 CO2 data, obtain the profiles of 1572 nm channel, with the geographic location and height corrected.	Profiles data of 1572 nm channel	HDF5
Level 2A	Attenuated backscatter coefficient with systematic constant correction	Attenuated backscatter coefficient	HDF5
Level 2B	Differential Absorption Optical Depth (DAOD) products	DAOD	HDF5
Level 2C	**Cloud and aerosol products including extinction coefficient, backscatter coefficient, depolarization ratio, AOD, lidar ratio and color ratio**	**Cloud and aerosol optical properties**	HDF5
Level 2D	XCO2	XCO2	HDF5

Chinese lidar ACDL/DQ-1: retrieval algorithm

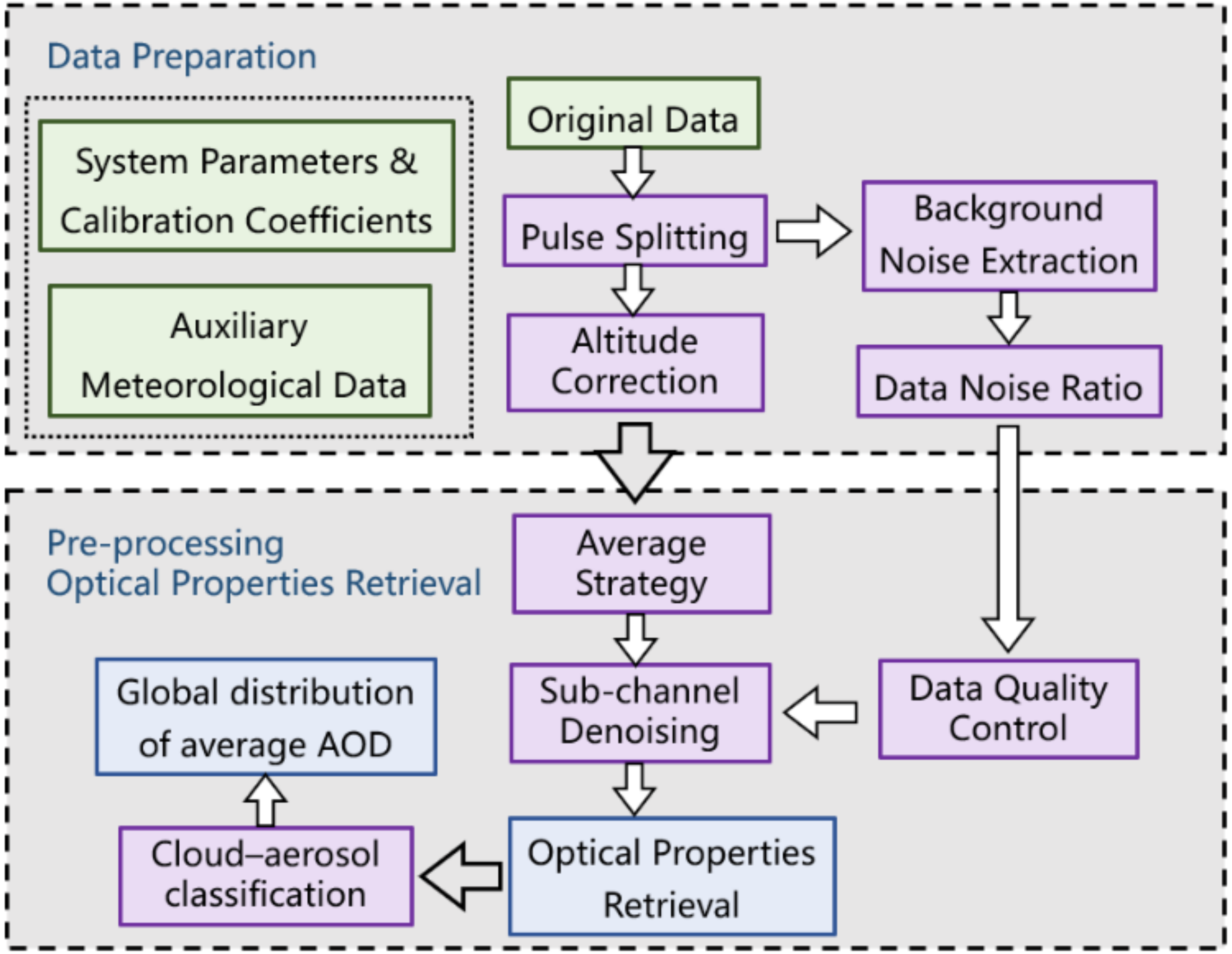

Chinese lidar ACDL/DQ-1: extinction coefficient

$$\alpha_a(z) = \frac{\partial \tau(z)}{\partial z} - \alpha_m(z)$$

nighttime

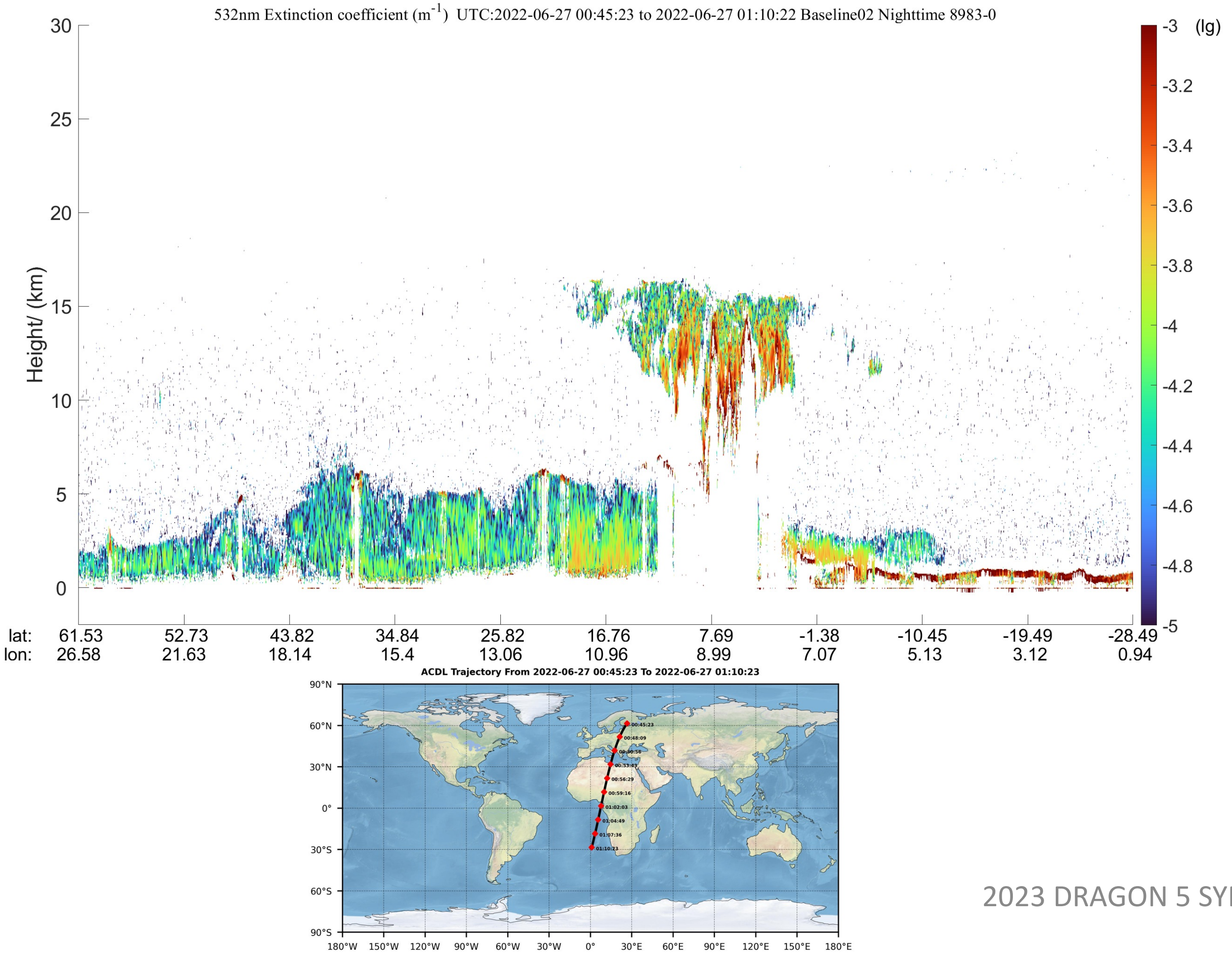

daytime

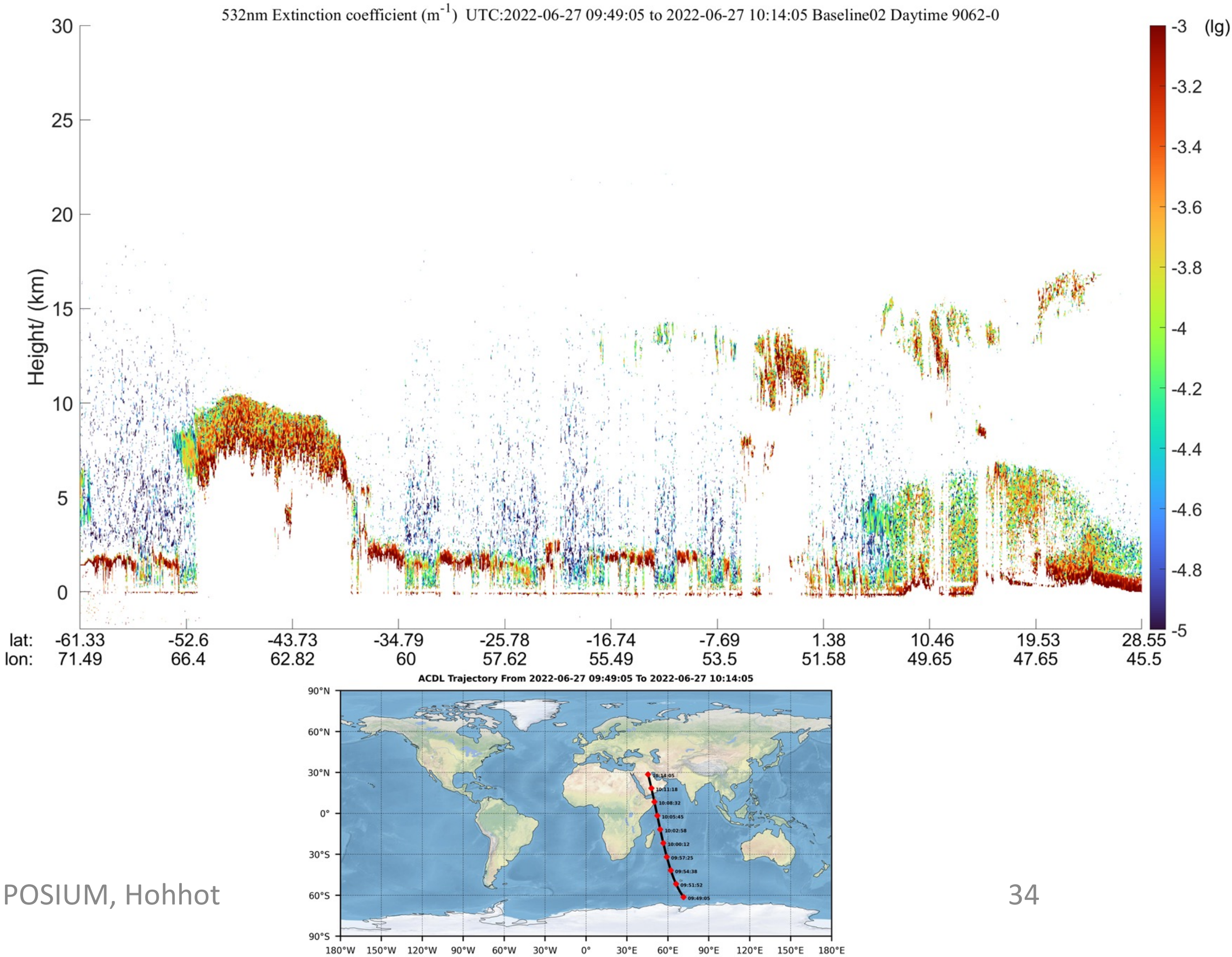

Chinese lidar ACDL/DQ-1: backscatter coefficient

$$\beta_a(z) = \beta_m(z)\frac{[1+\delta(z)][f_m(z)-f_a]\mathcal{R}(z)}{(1+\delta_m)[1-f_a\mathcal{R}(z)]} - \beta_m(z)$$

nighttime

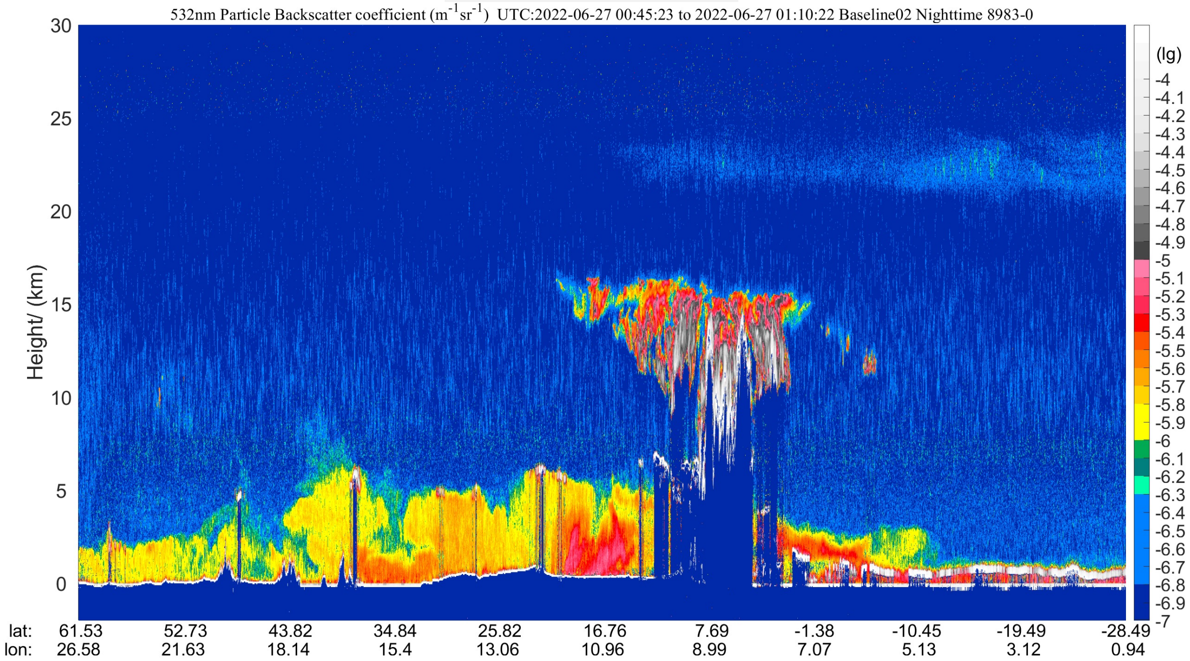

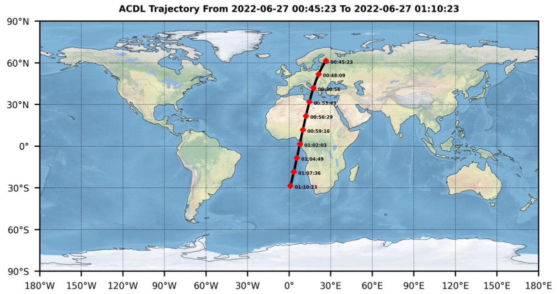

daytime

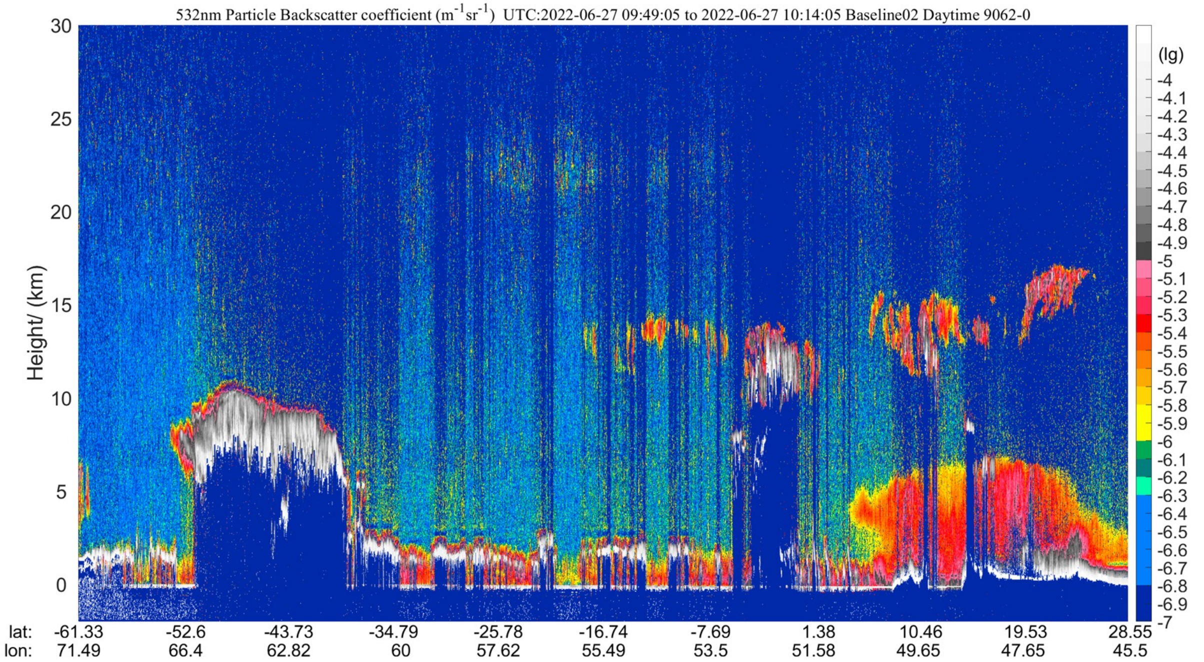

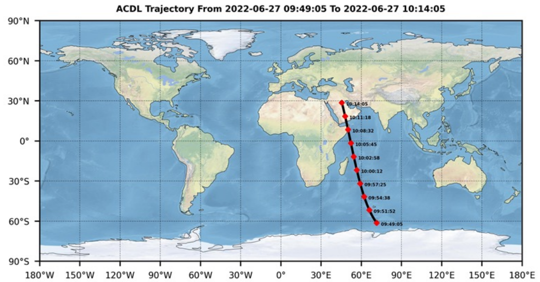

Chinese lidar ACDL/DQ-1: total depolarization ratio

$$\delta(z) = \frac{\beta_m^{\perp}(z)+\beta_a^{\perp}(z)}{\beta_m^{\parallel}(z)+\beta_a^{\parallel}(z)} = \frac{P^{\perp}(z,\lambda)C^{\parallel}K^{\parallel}}{P^{\parallel}(z,\lambda)C^{\perp}K^{\perp}}.$$

- describe the shape characteristics of the aerosol particles
- related to the degree of regularity of the particle shape

nighttime

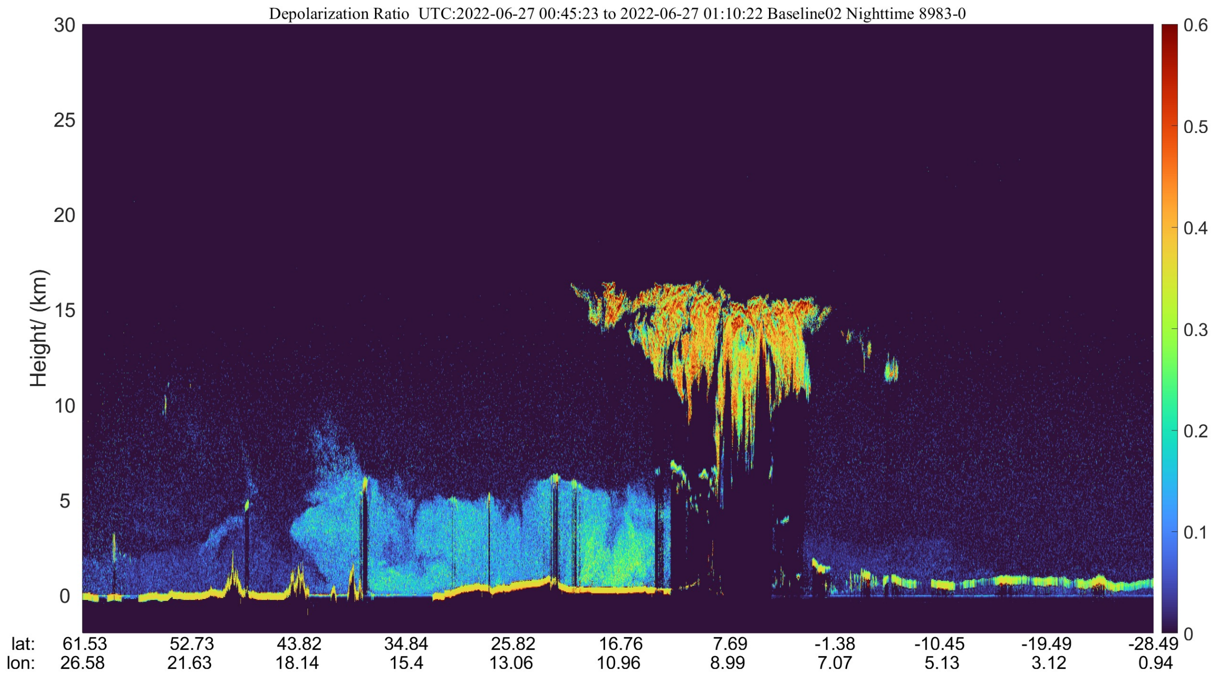

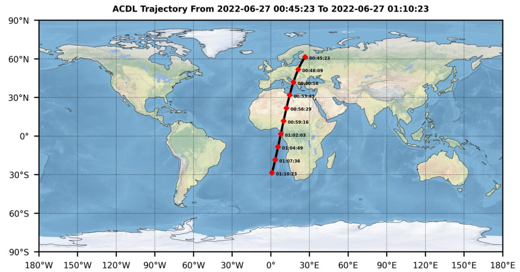

daytime

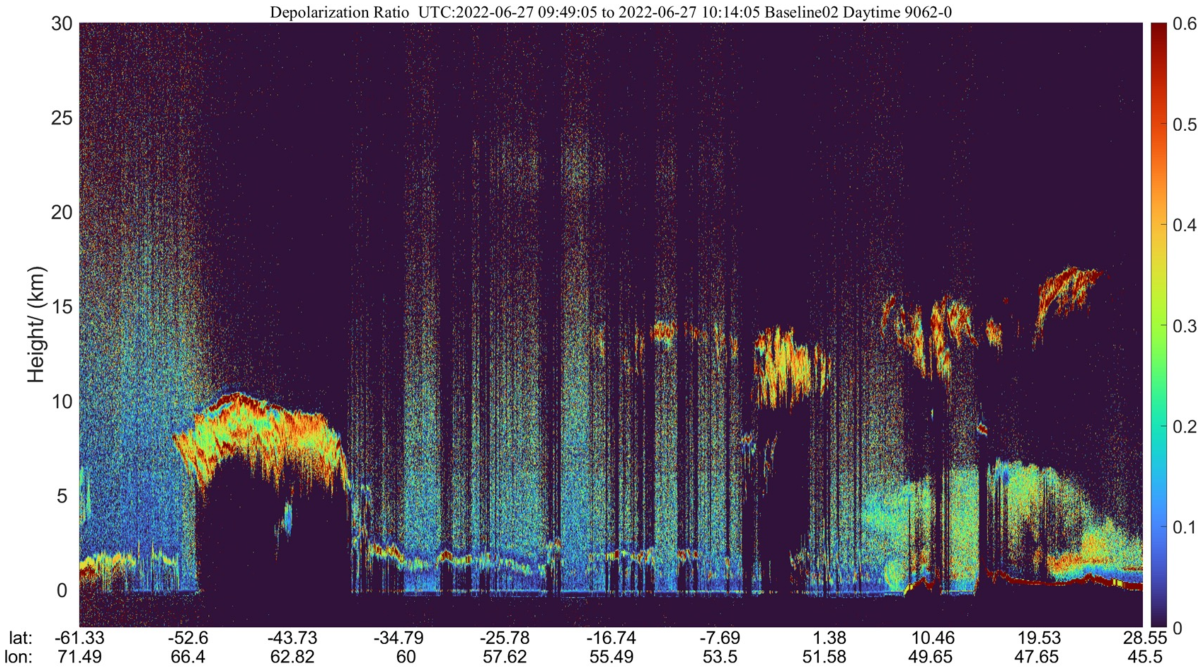

Chinese lidar ACDL/DQ-1: lidar ratio

$$S_a(z) = \frac{\alpha_a(z)}{\beta_a(z)}$$

- an important parameter to distinguish the aerosol types

nighttime

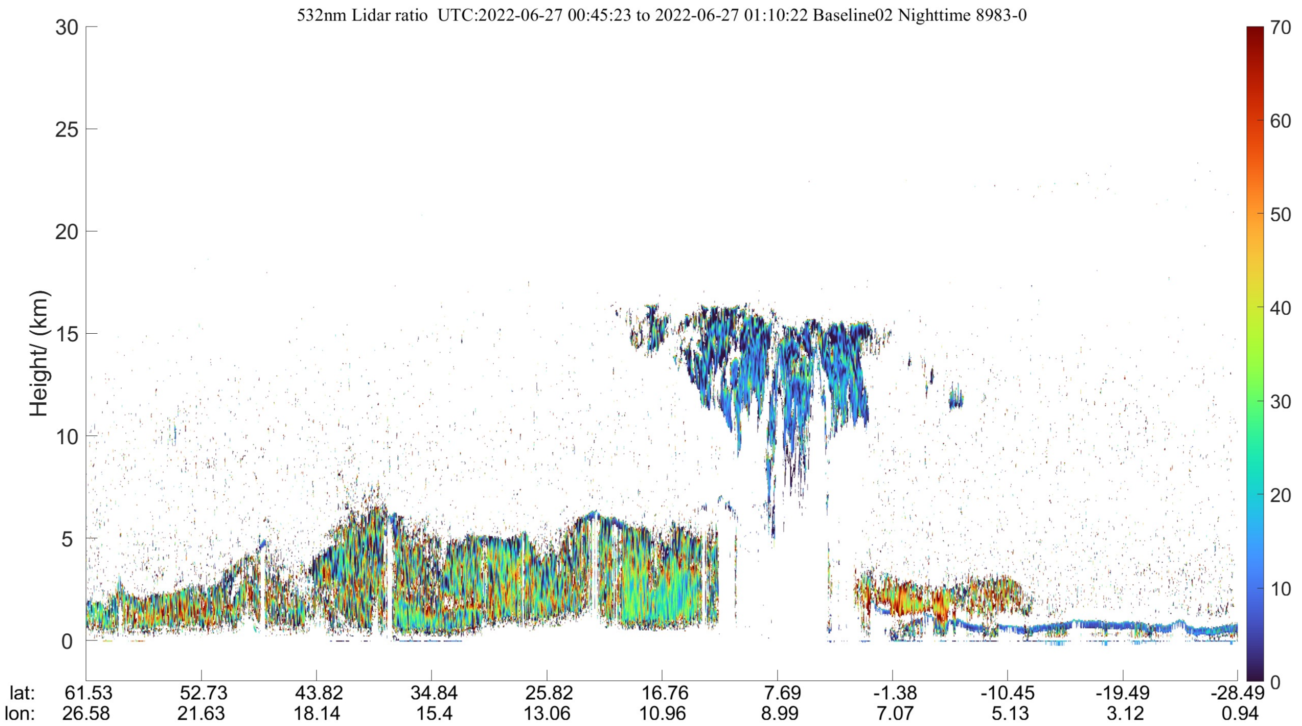

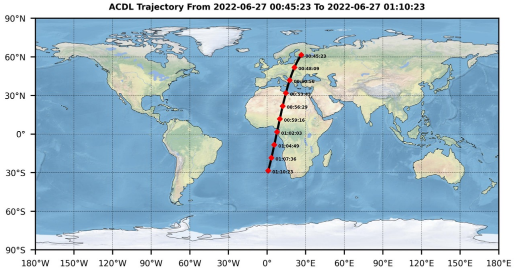

daytime

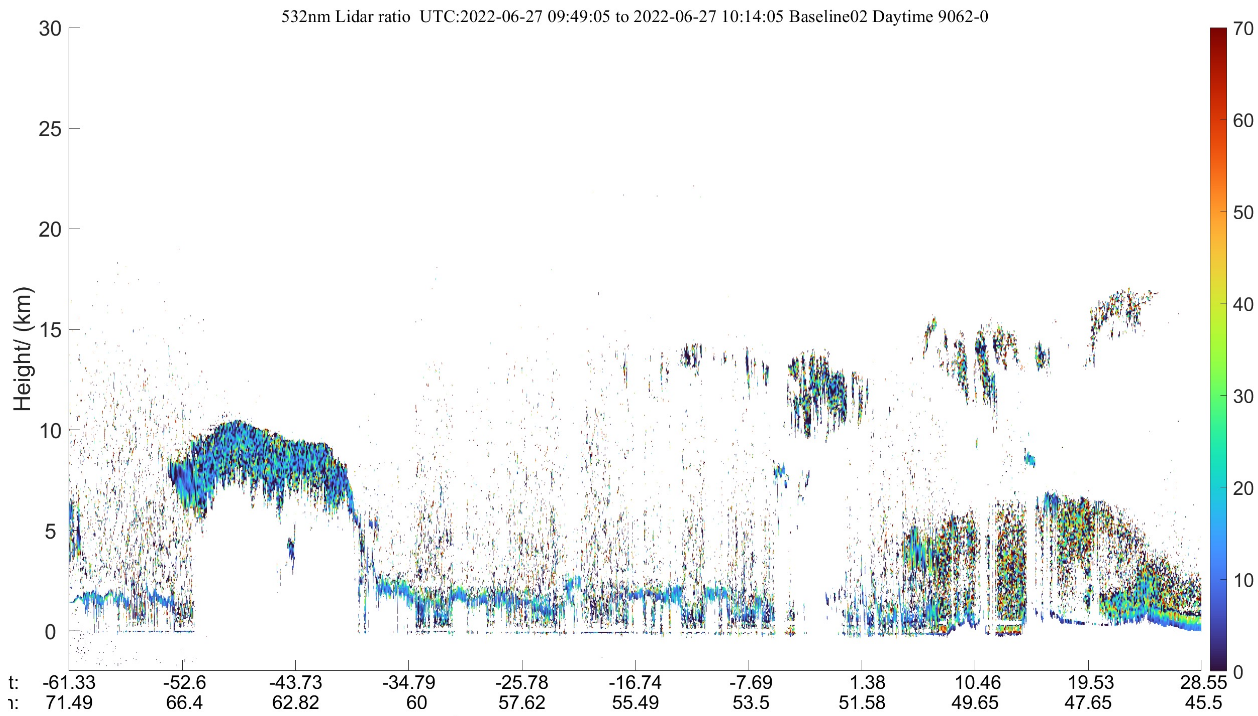

Chinese lidar ACDL/DQ-1
Measurement case: Central Asia-South Asia-Indian Ocean

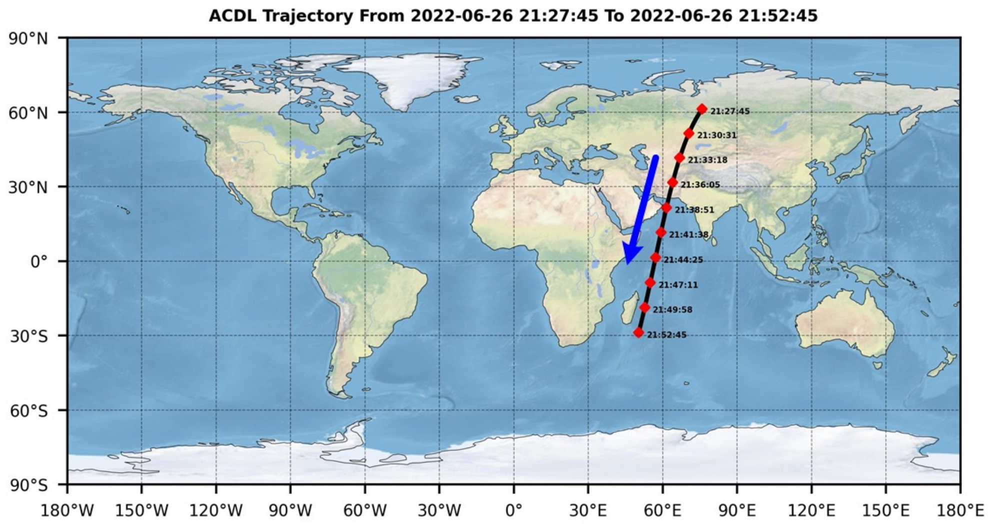

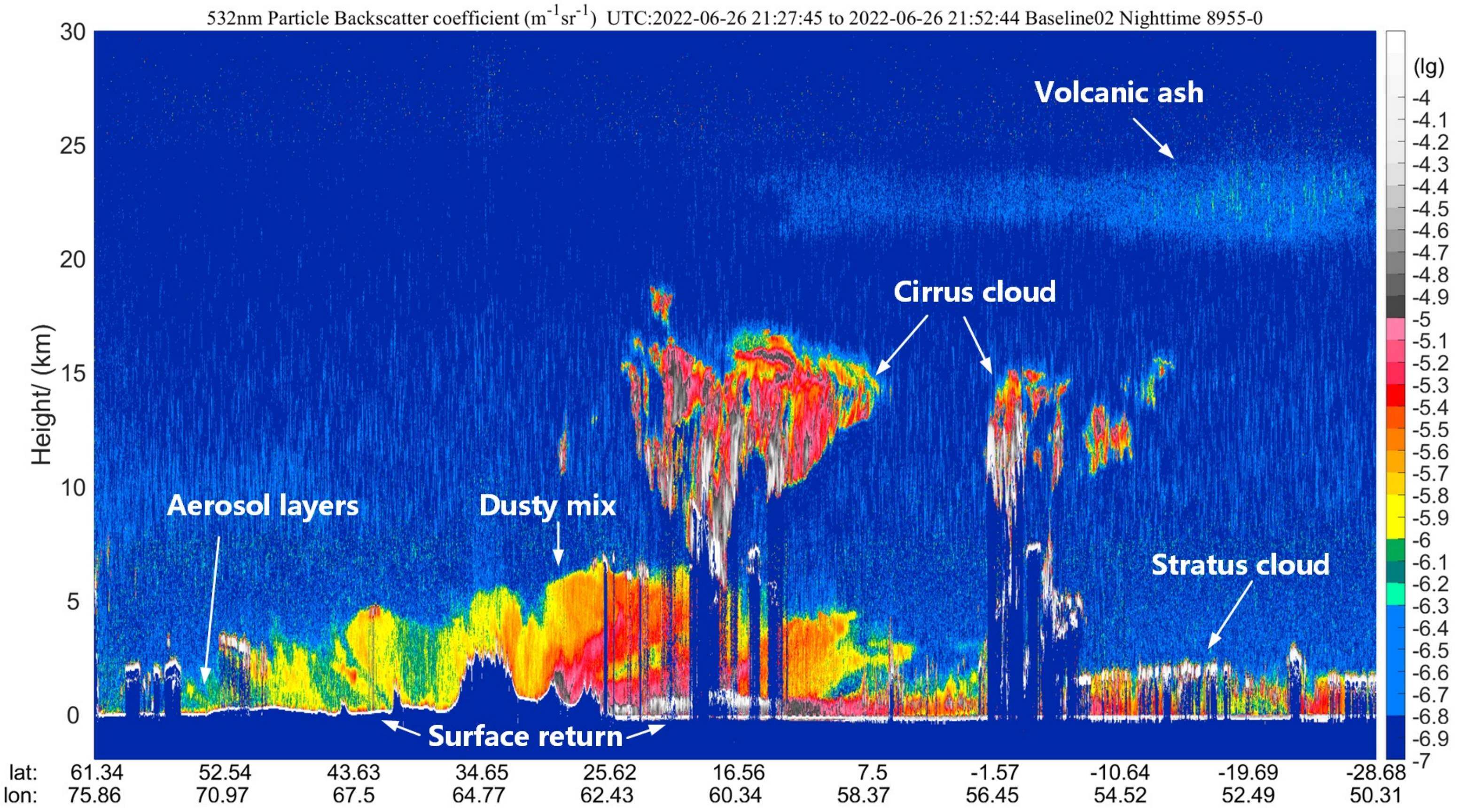

European Young scientists contributions in Dragon 5

Name	Institution	Poster title	Contribution
Oliver Lux	DLR		Aeolus calibration and validation

Chinese Young scientists contributions in Dragon 5

Name	Institution	Poster title	Contribution
Kangwen Sun	OUC	Correlation Between Marine Aerosol Optical Properties and Wind Fields over Remote Oceans with Use of Aeolus Observations	Aeolus validation and application, ACDL data retrieval
Xiaoying Liu	OUC		Aeolus validation

☐ Summary

- **ESA's lidar ALADIN/Aeolus**
  - ➢ Accomplished the calibration and validation of Aeolus data, evaluated the data quality.
  - ➢ Explored the scientific application of Aeolus products on aerosol observation.
- **Chinese lidar ACDL/DQ-1**
  - ➢ Preliminarily established the aerosol and cloud optical properties retrieval algorithm.

THANK YOU!